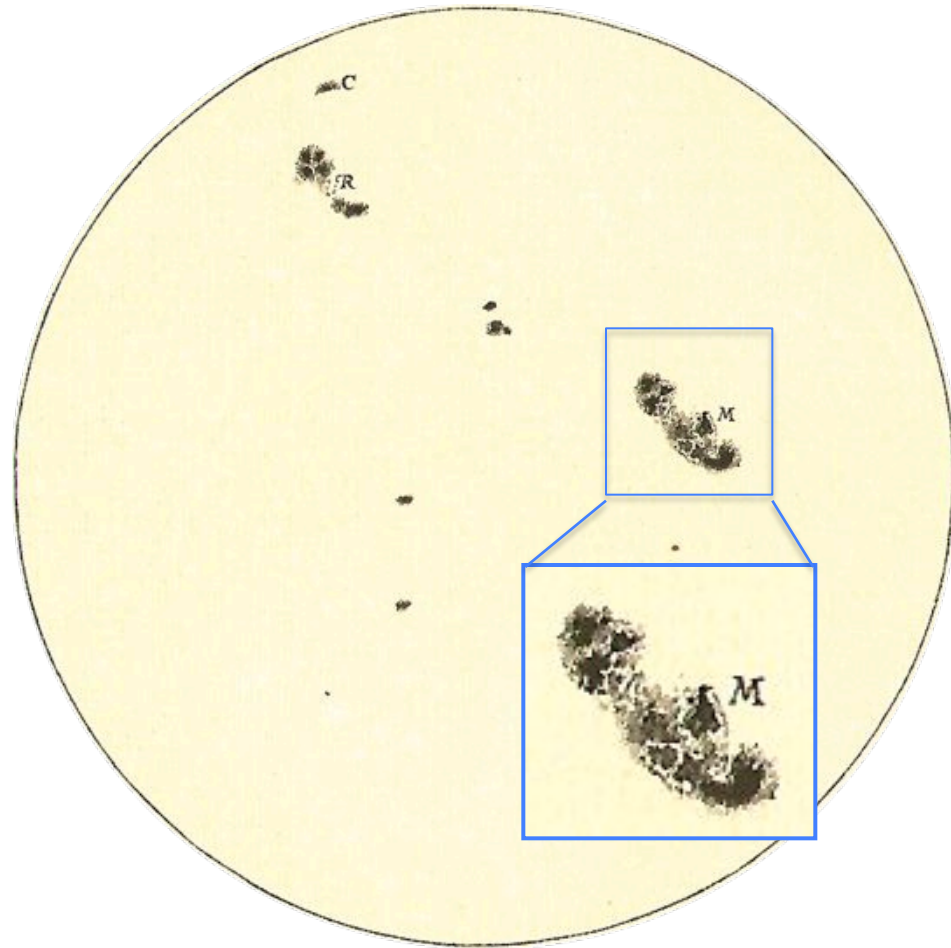


Cap. 11 – O Sol

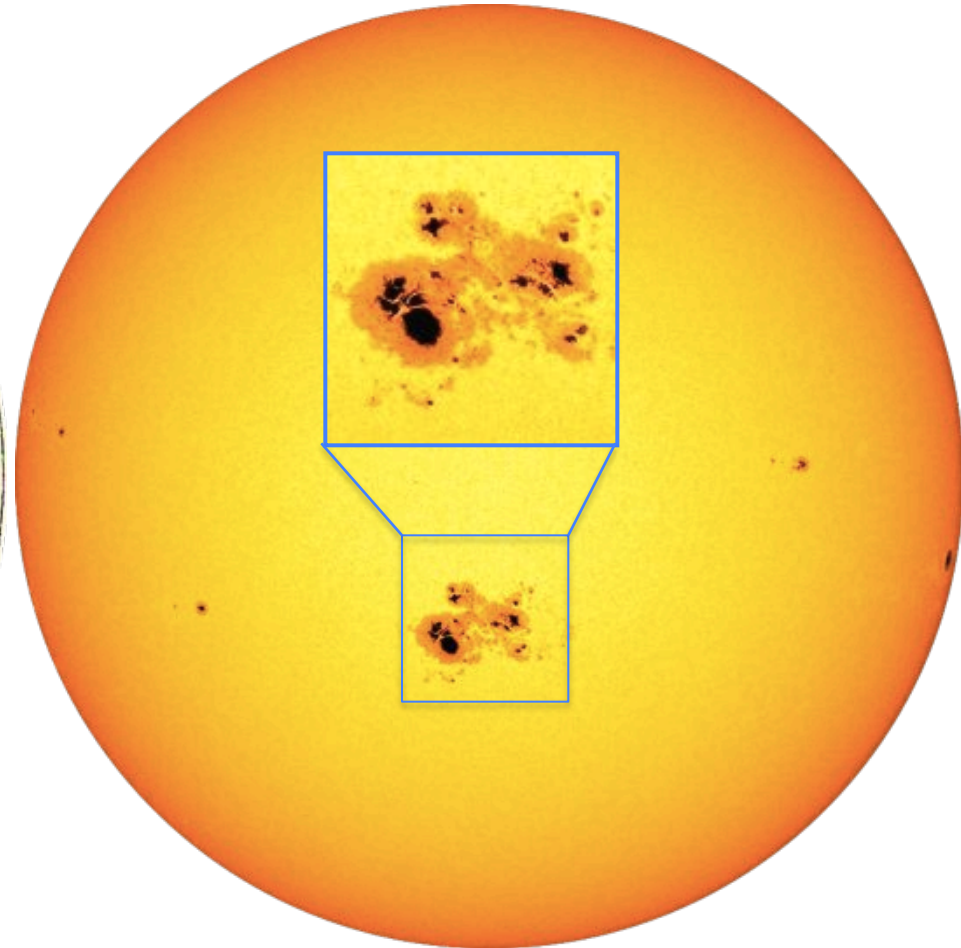
11.3 O ciclo de atividade solar

Dr. Jorge Meléndez
AGA 0293, Astrofísica Estelar

Manchas solares



23/6/1613
Galileu Galilei



23/10/2014
NASA/SDO

22/6/1613

27/6/1613

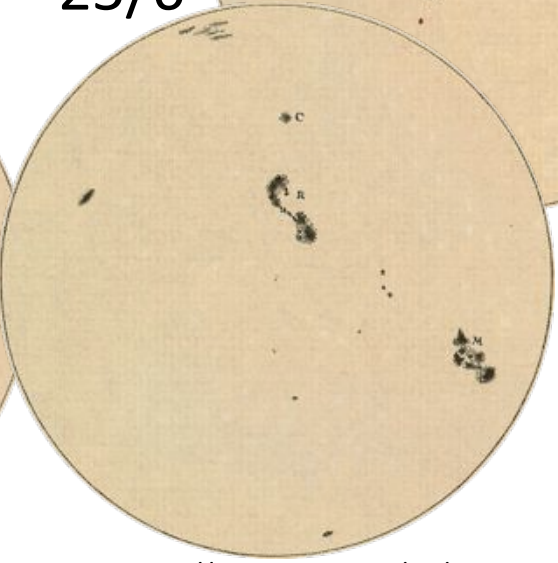
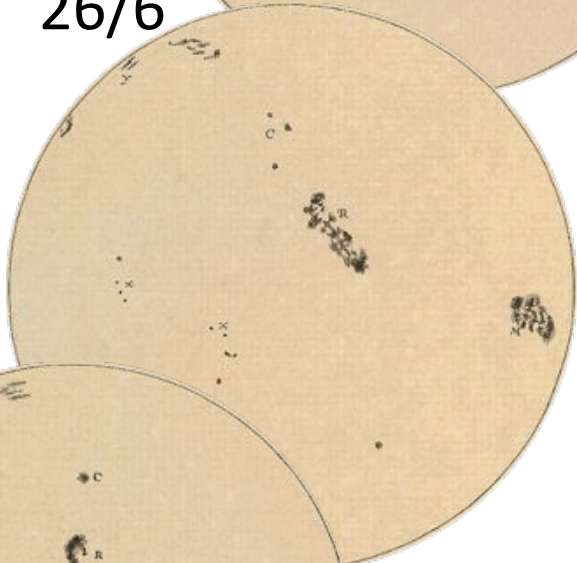
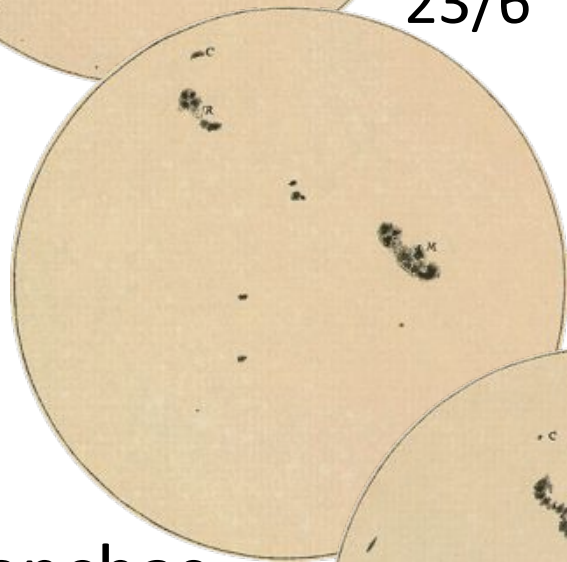
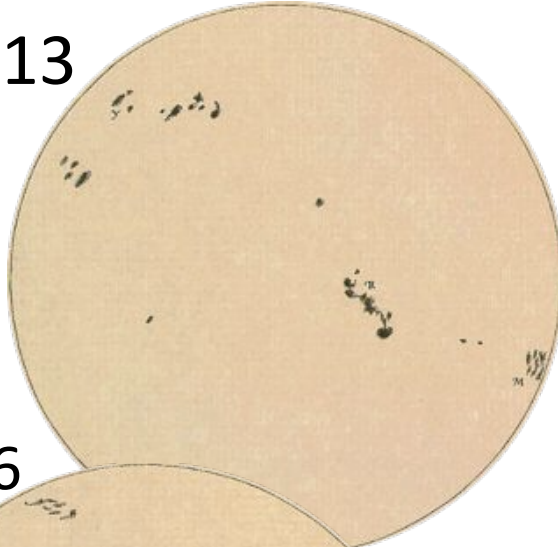
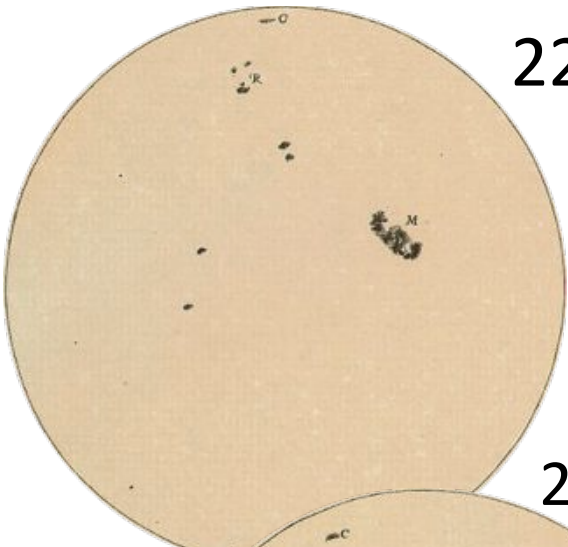
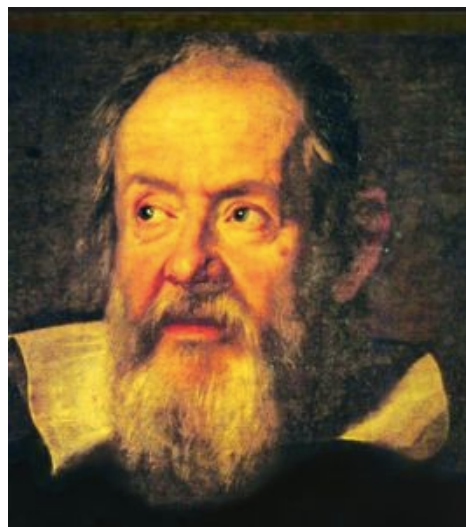
23/6

26/6

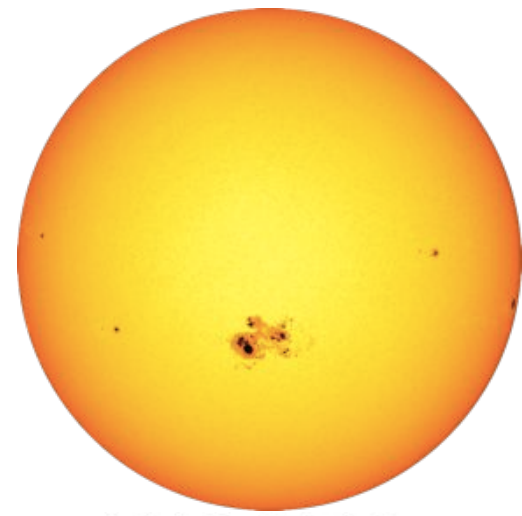
24/6

25/6

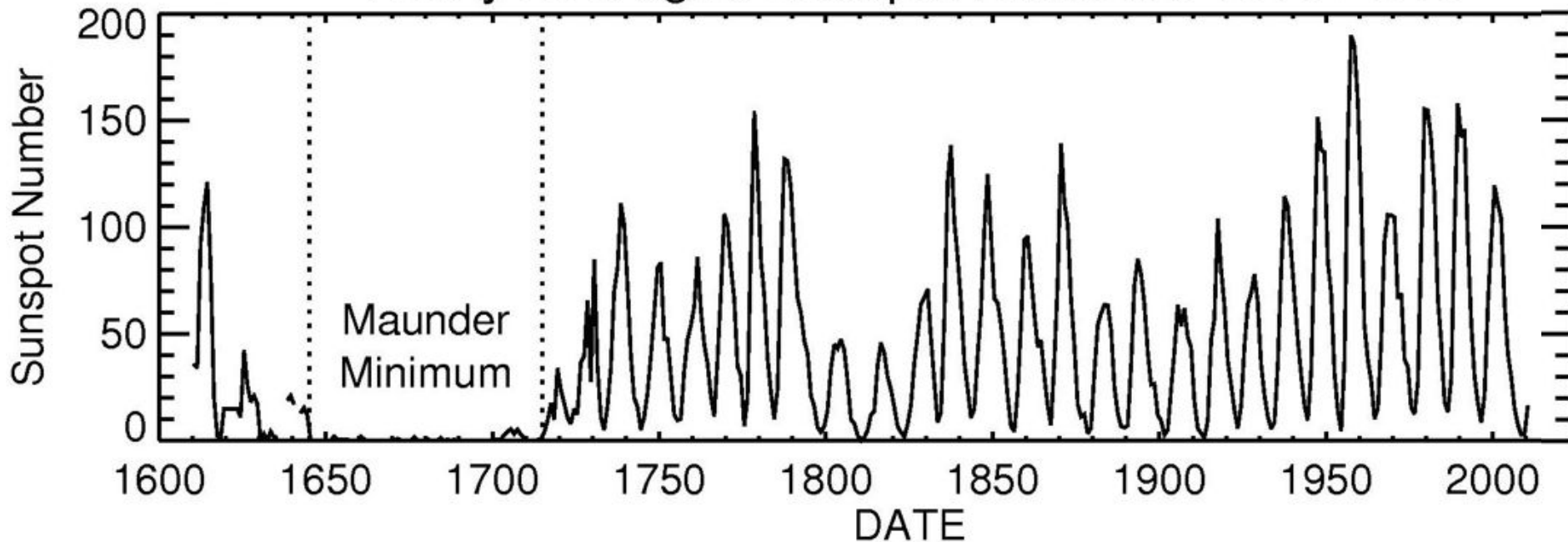
Manchas
solares
observadas
por Galileu



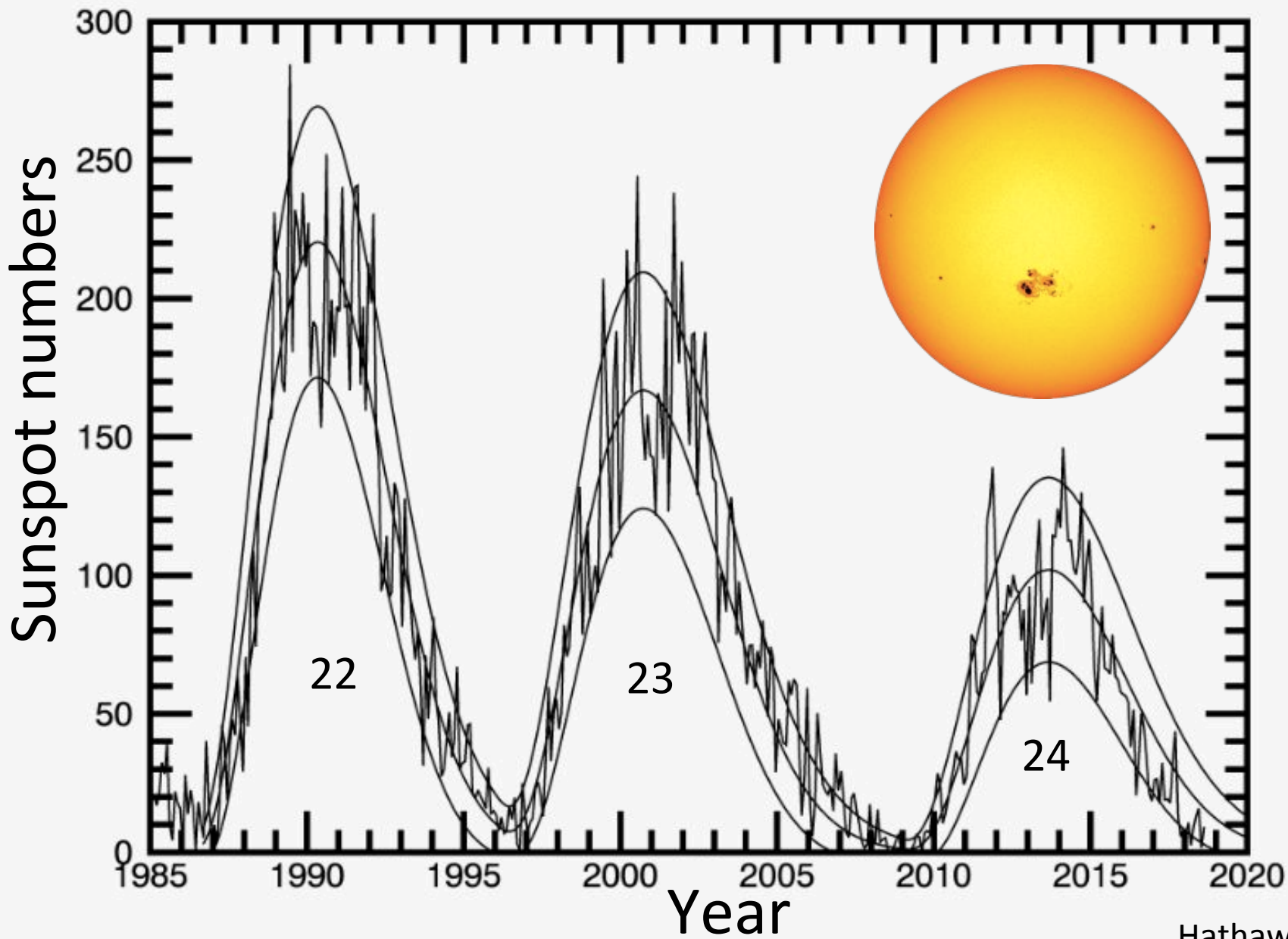
Ciclo de manchas solares quase periódico ~ 11 anos



Yearly Averaged Sunspot Numbers 1610-2010

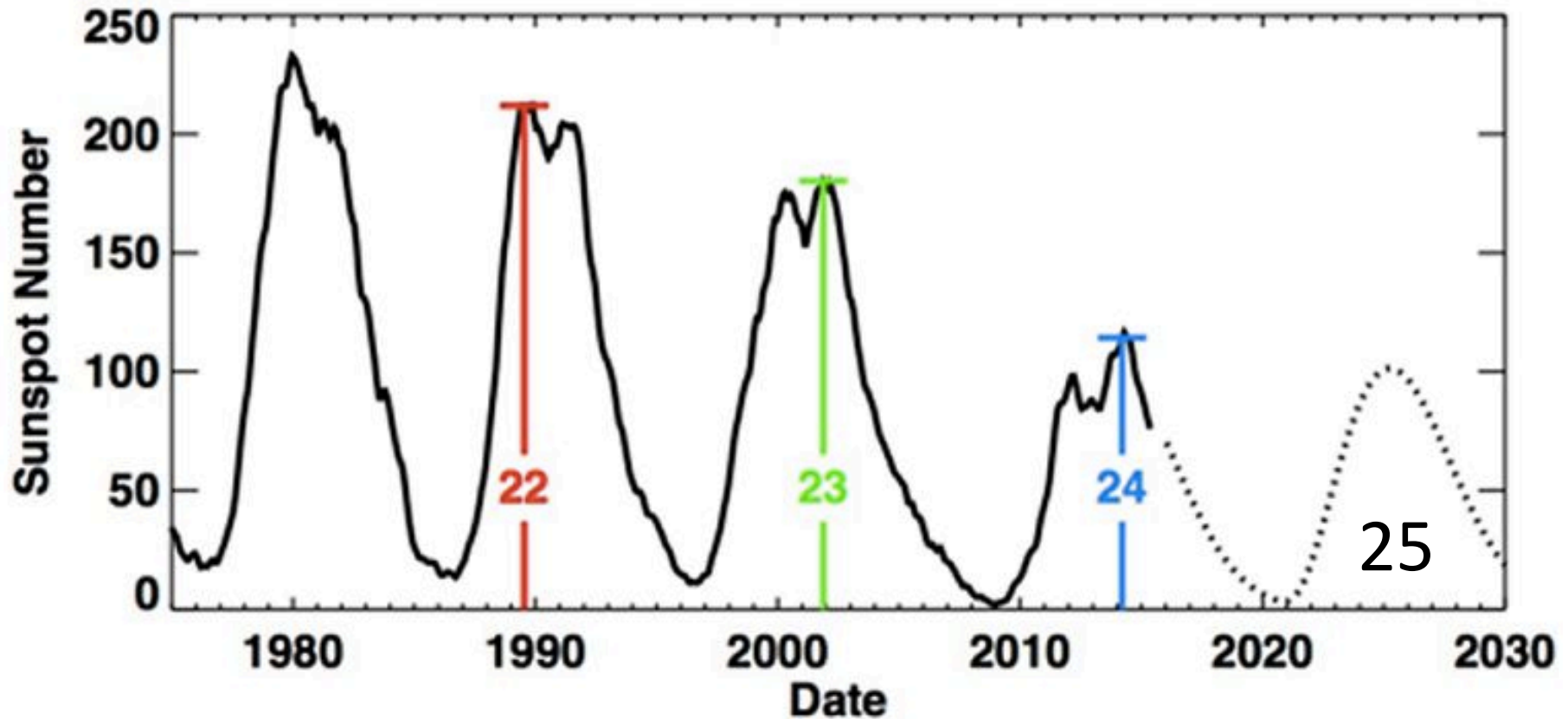


Cycle 24 Sunspot Number (V2.0) Prediction (2018/9)

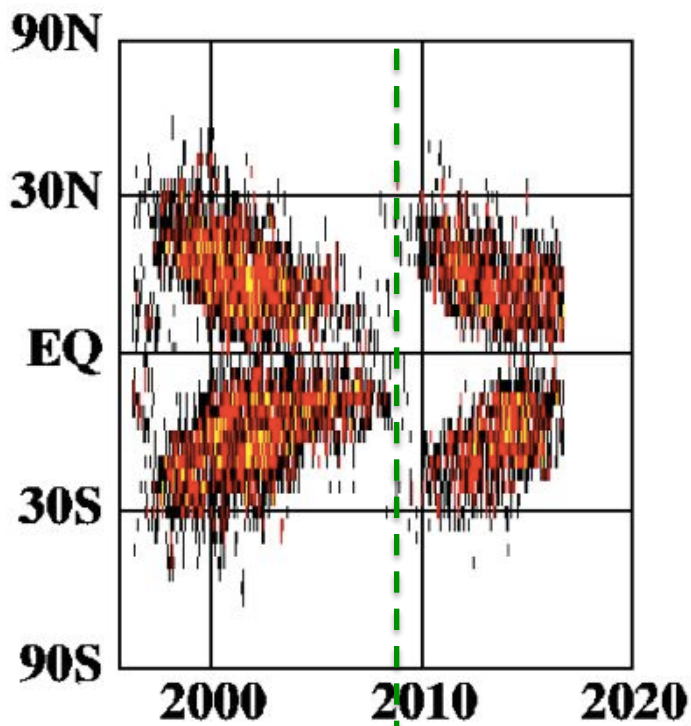


Hathaway

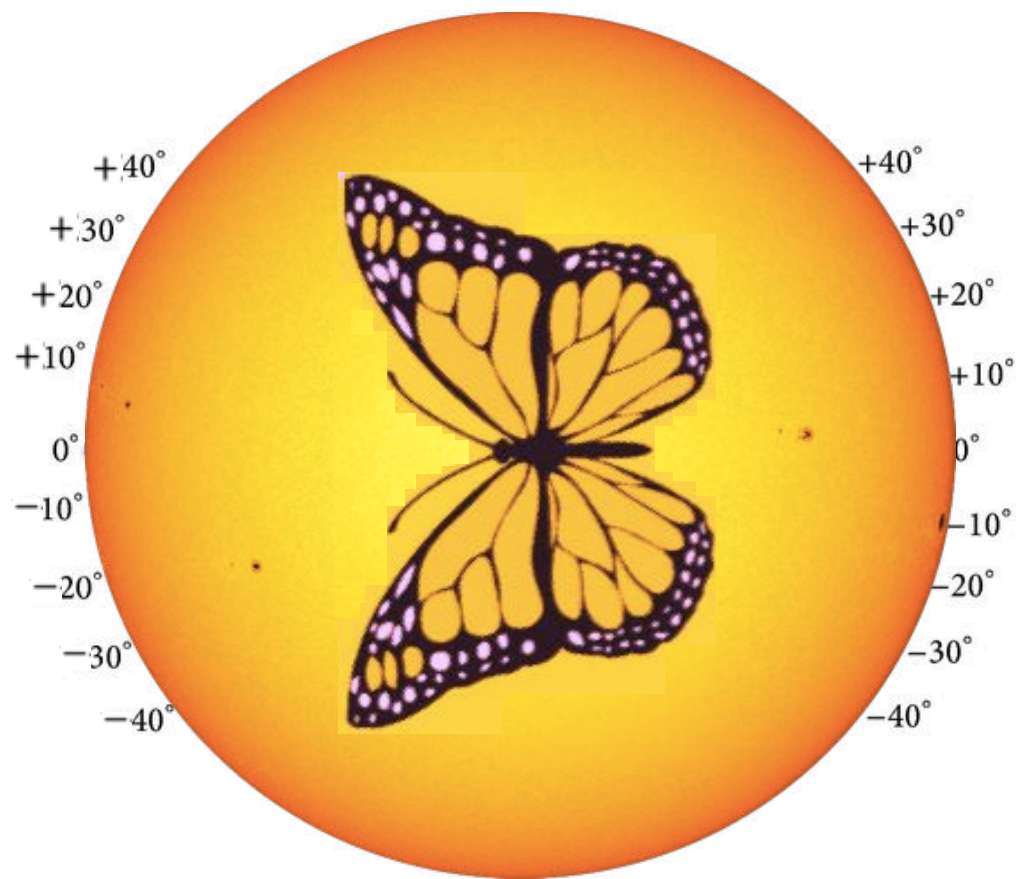
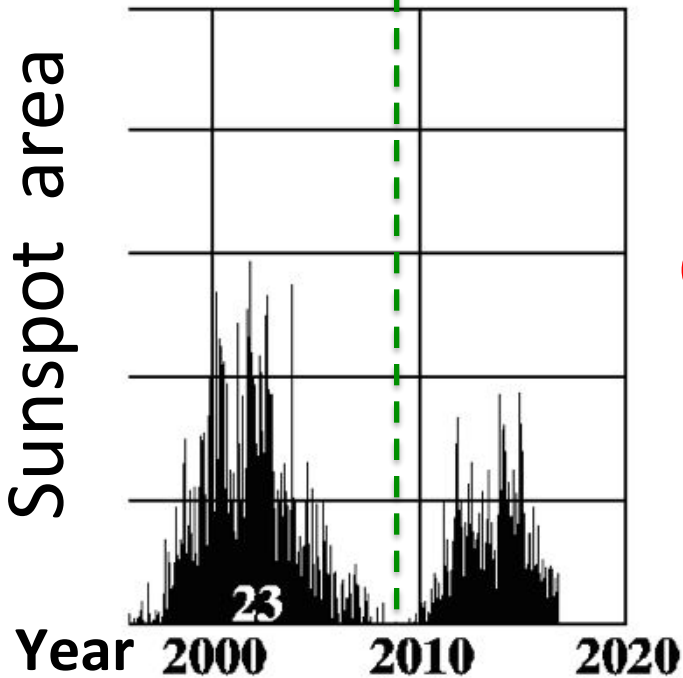
Previsão do ciclo solar 25



Solar latitude



Sunspot area



Butterfly diagram

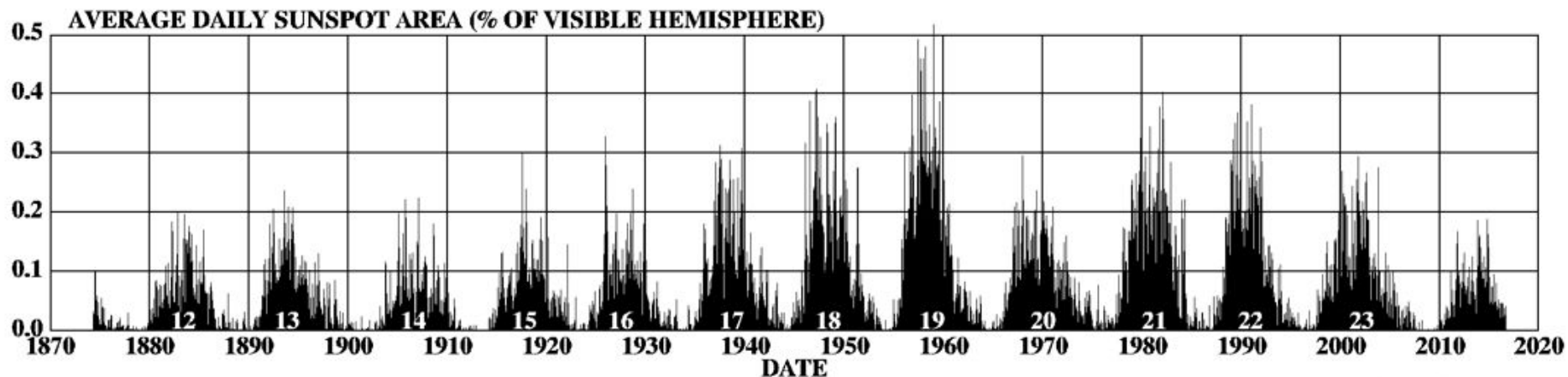
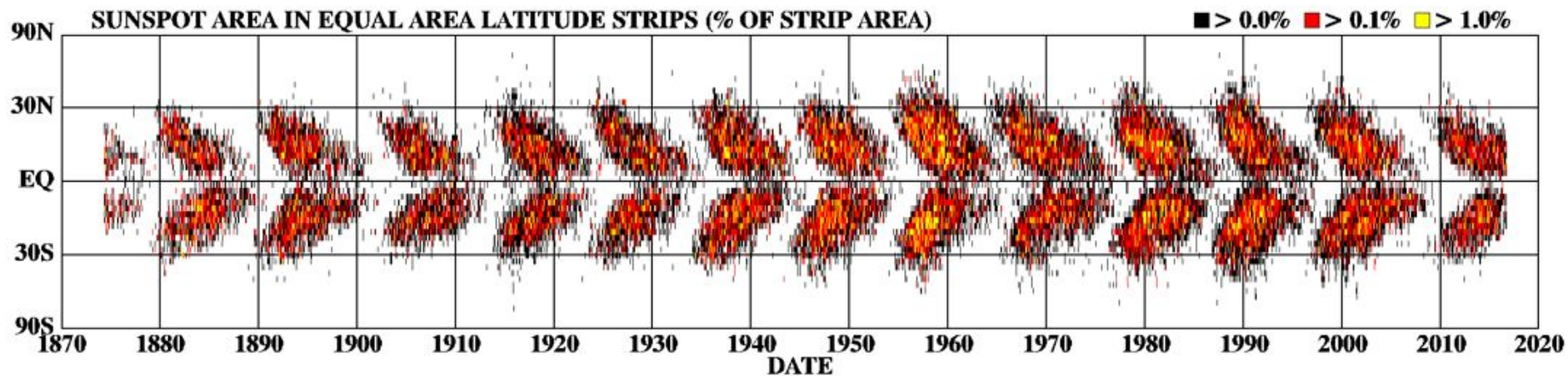
Começa ciclo: altas latitudes ($\pm 40^\circ$)

Fim do ciclo: perto do equador

Butterfly diagram

Começo do ciclo: altas latitudes $\pm 40^\circ$. Fim do ciclo: perto do equador

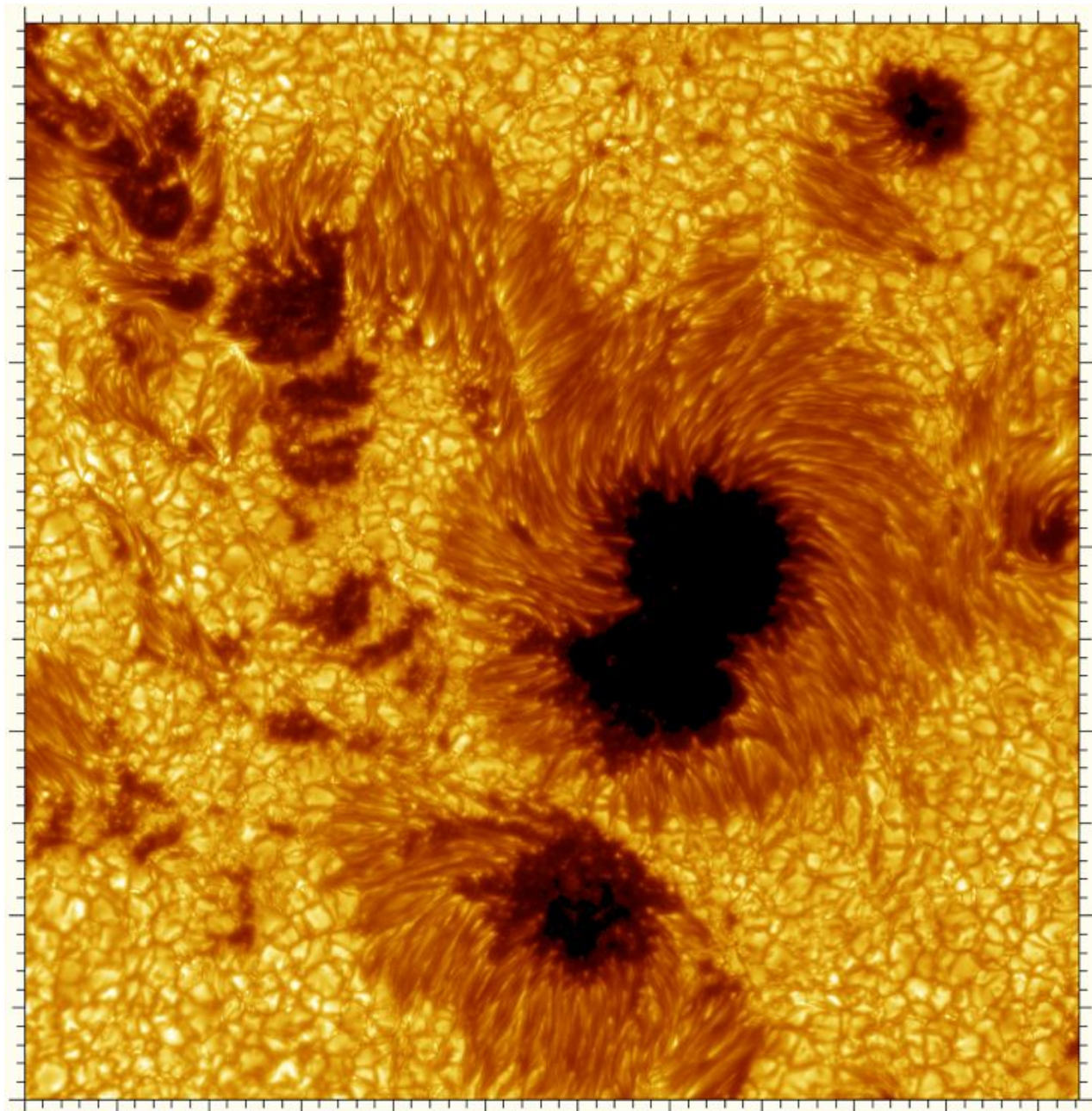
DAILY SUNSPOT AREA AVERAGED OVER INDIVIDUAL SOLAR ROTATIONS





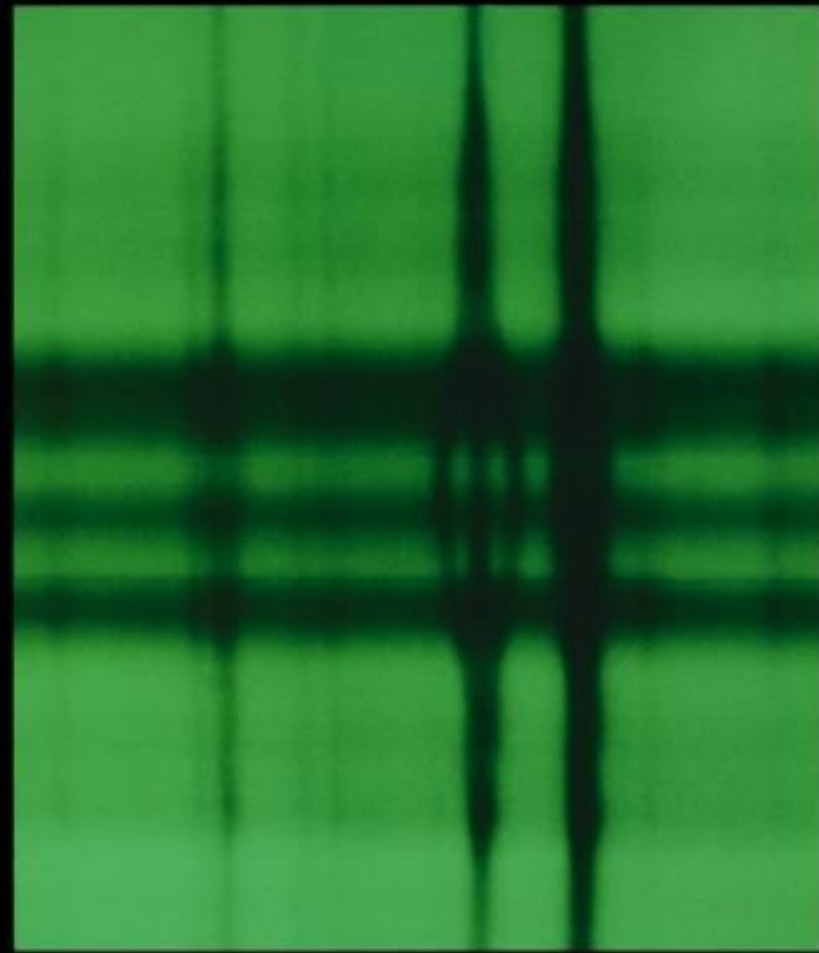
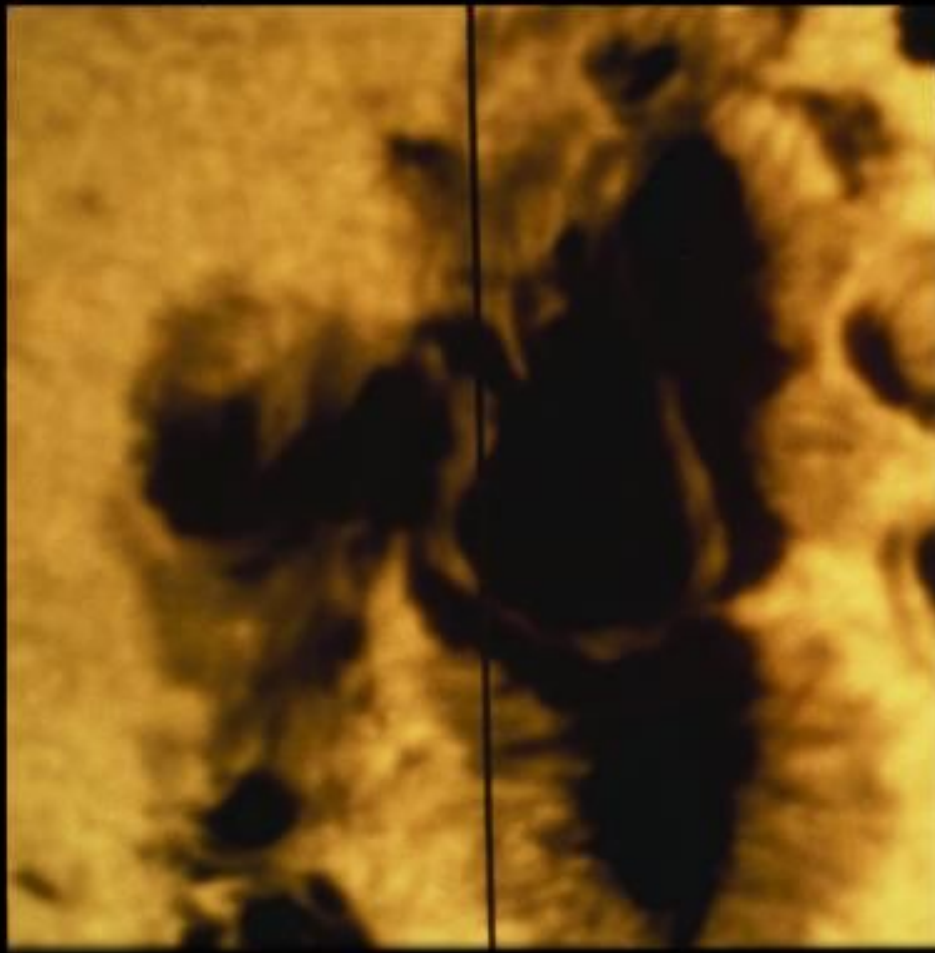
Umbra: região mais escura.

Penumbra: região um pouco mais clara e com estrutura filamentar, que sugere linhas de campos magnéticos.



Nota: além dos grânulos, é possível observar algumas fáculas (pontos brilhantes)

Sunspots observed on 15 July 2002.
The distance between 2 ticks is 1000 km



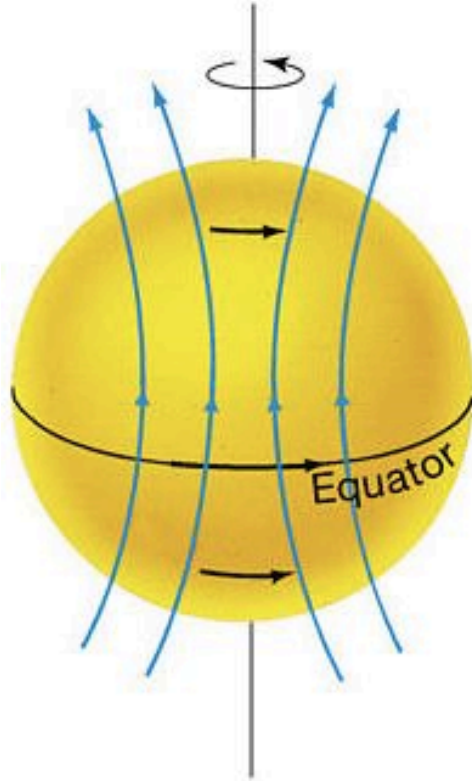
The vertical black line on the **left** indicates the location of the slit for the spectrograph which took the spectrum (**right**). The division of 1 spectral line into 3 demonstrates the Zeeman effect. The splitting of this iron line at 5250.2 \AA , indicates a field strength of 4130 Gauss.

© McMath-Pierce Solar Facility on Kitt Peak.

https://www.noao.edu/image_gallery/html/im0404.html

Ciclo de manchas solares

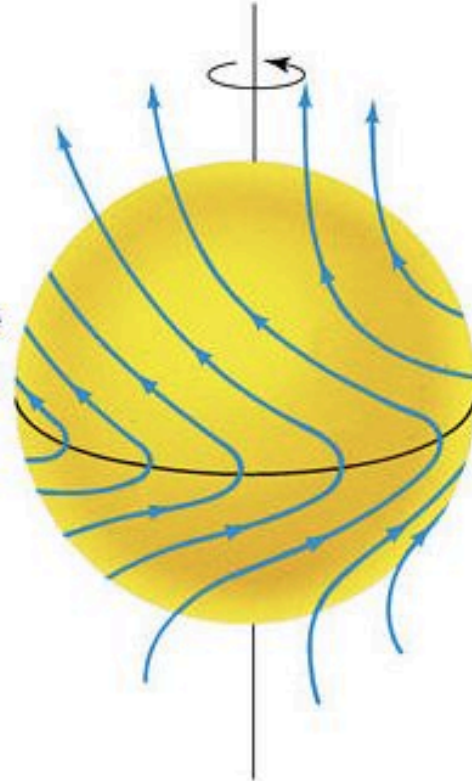
Campo poloidal



Time



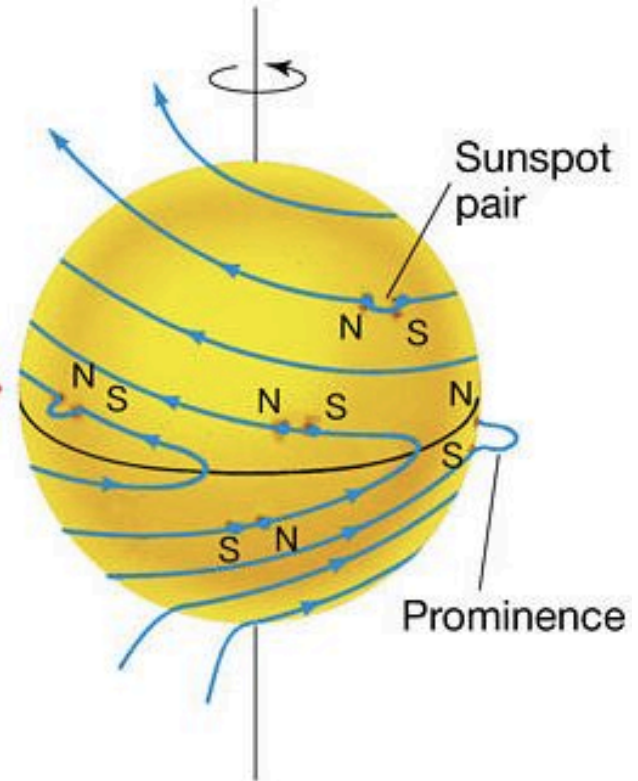
North Pole



South Pole

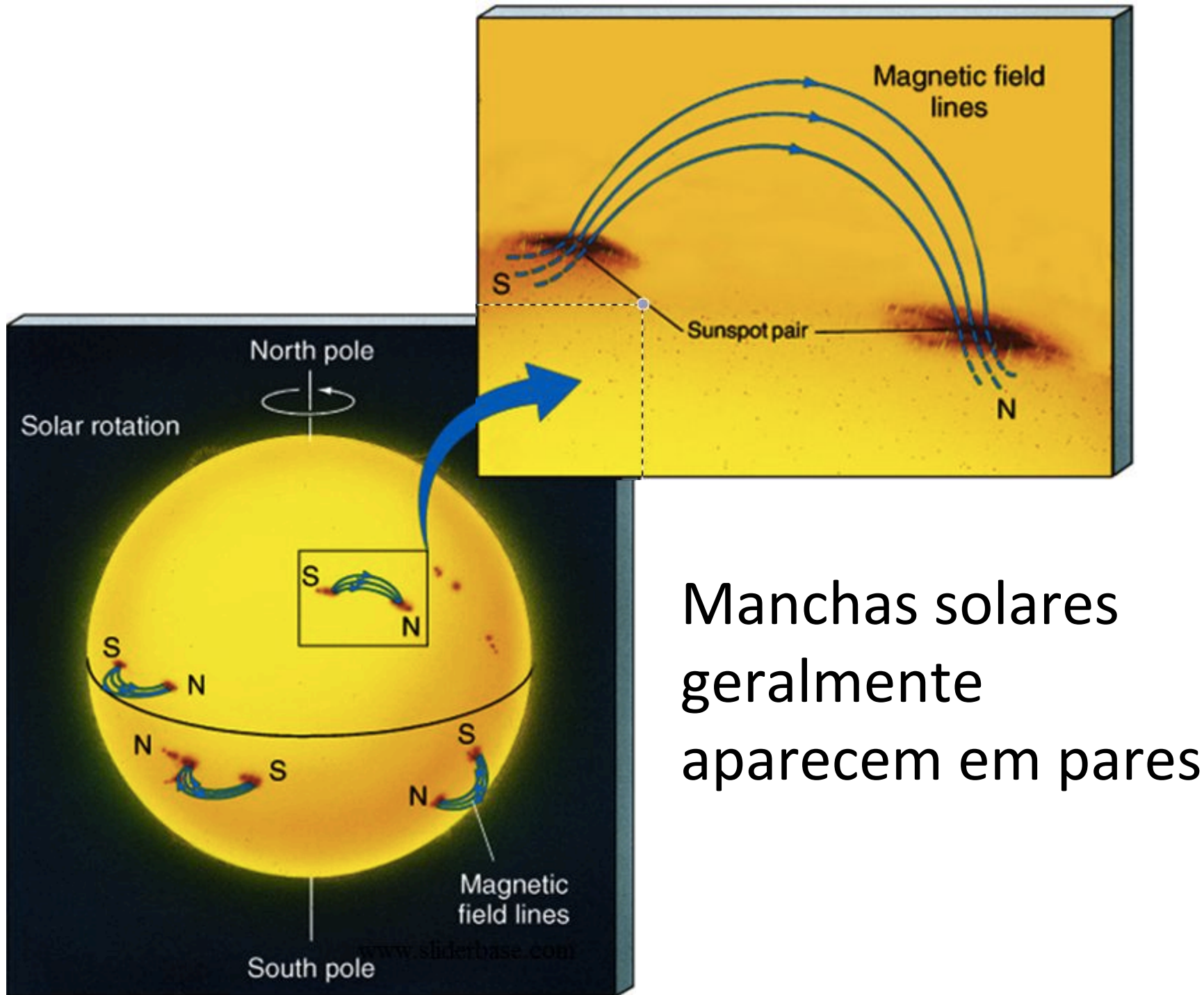


Campo toroidal



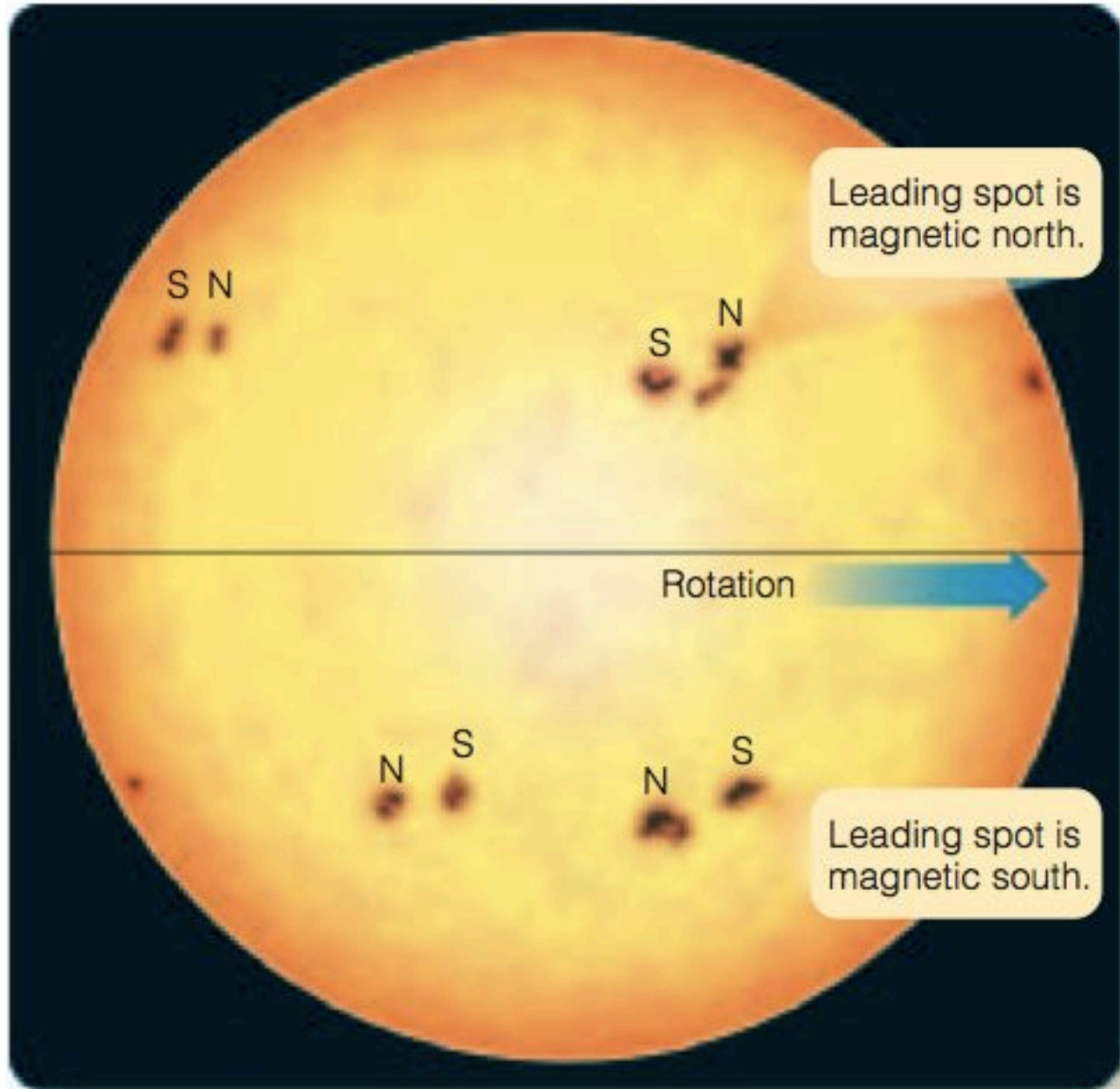
Copyright © 2005 Pearson Prentice Hall, Inc.

Linhas de campo magnético mais enroladas
→ manchas solares



Manchas solares
geralmente
aparecem em pares

In sunspot groups, here simplified into pairs of major spots, the leading spot and the trailing spot have opposite magnetic polarity. Spot pairs in the southern hemisphere have reversed polarity from those in the northern hemisphere.



Ciclo magnético: 22 anos

Campo poloidal é invertido a cada 11 anos, e volta após 22 anos

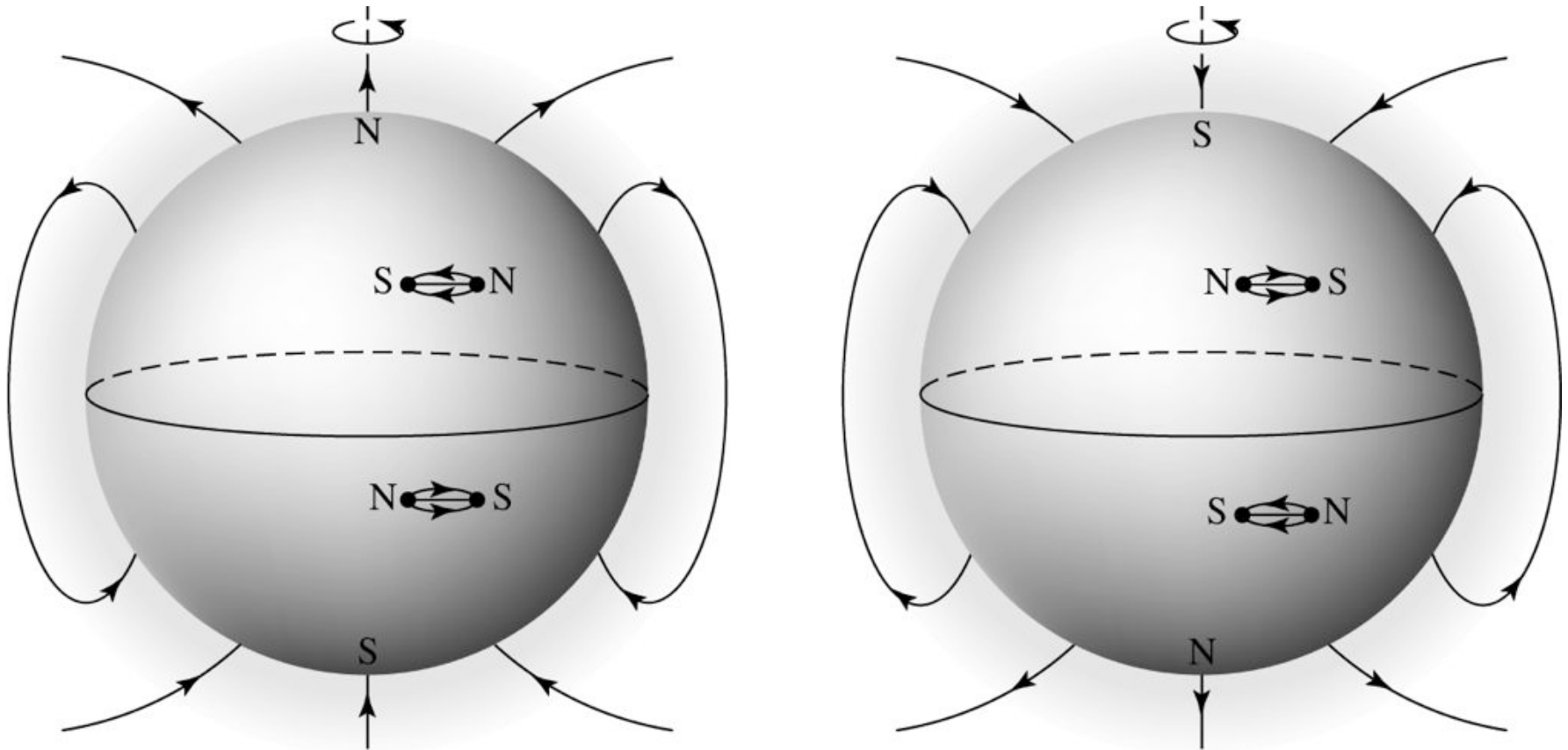


FIGURE 11.32 The global magnetic field orientation of the Sun, along with the magnetic polarity of sunspots during successive 11-year periods.

Magnetic fields trap gas:

$$F_{\text{surf}} = \sigma T_e^4$$

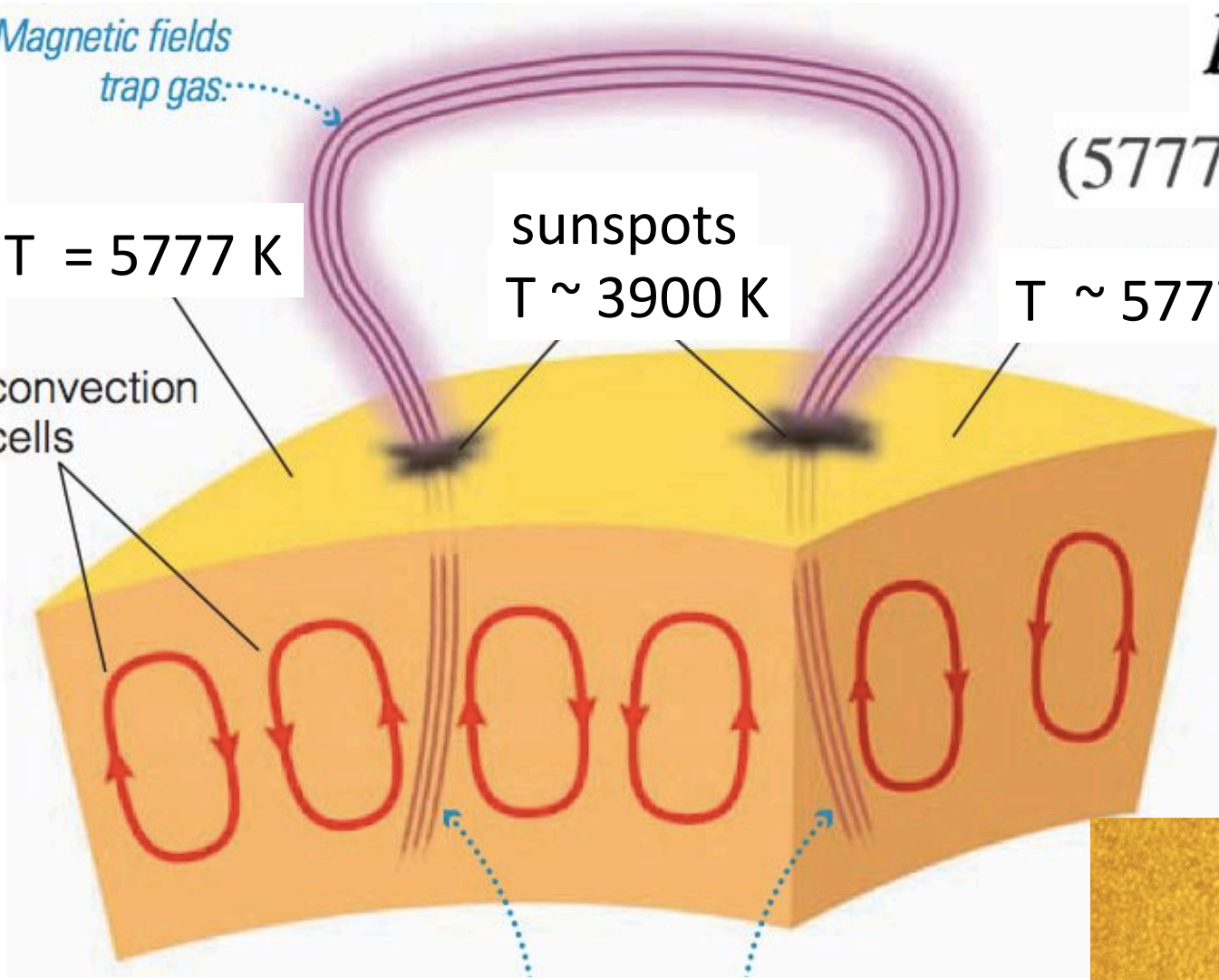
$$(5777/3900)^4 = 4.8$$

T = 5777 K

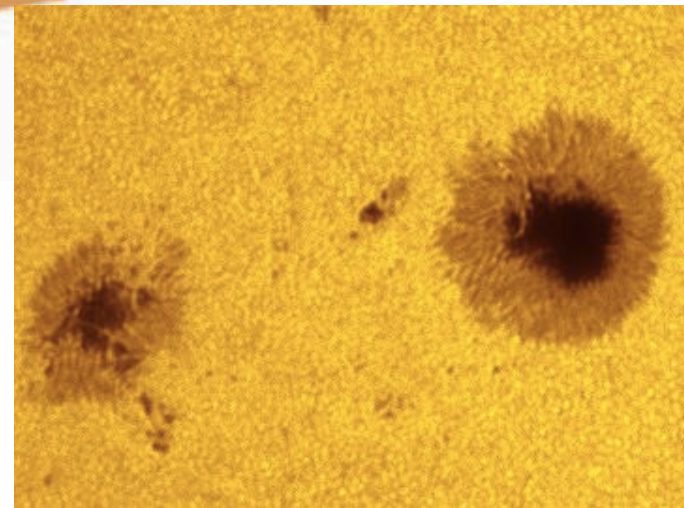
sunspots
T ~ 3900 K

T ~ 5777 K

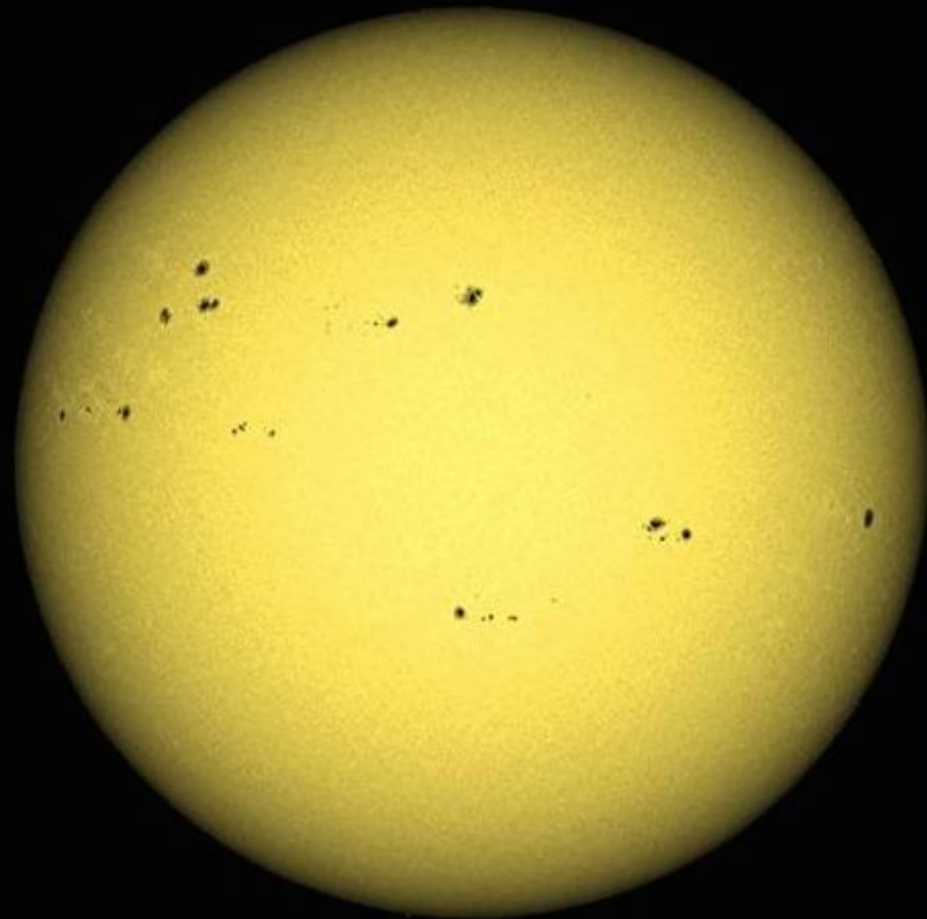
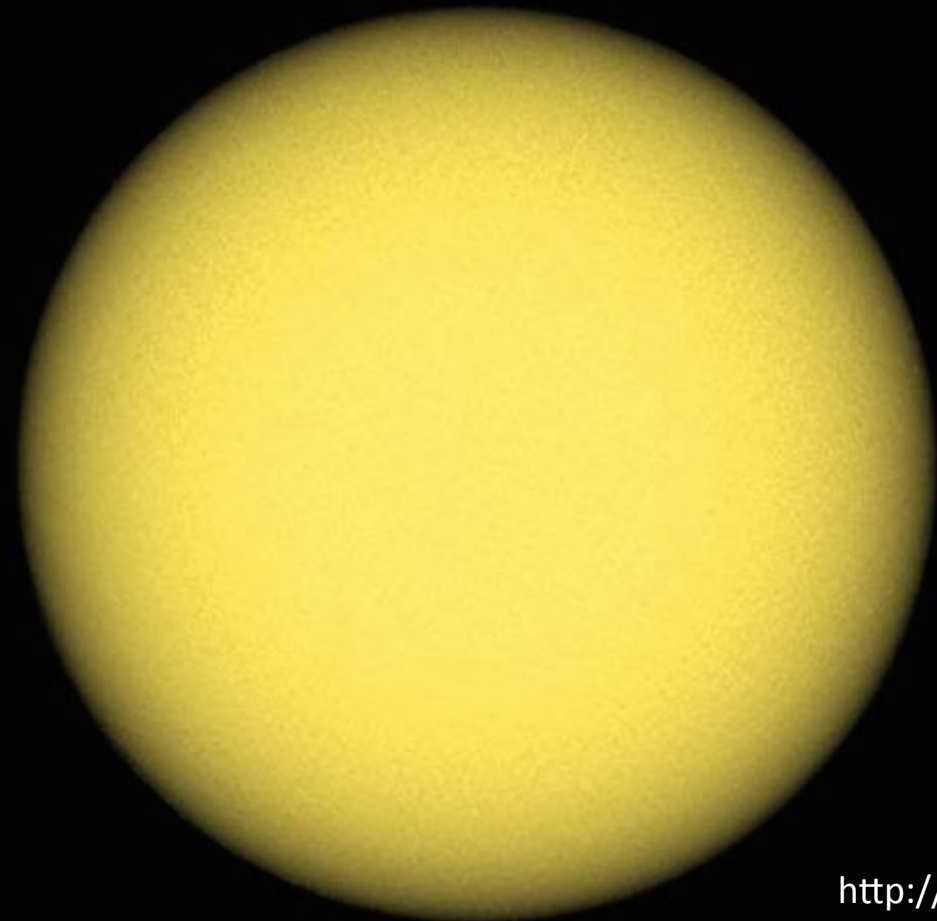
convection cells



Magnetic fields of sunspots suppress convection and prevent surrounding plasma from sliding sideways into sunspot

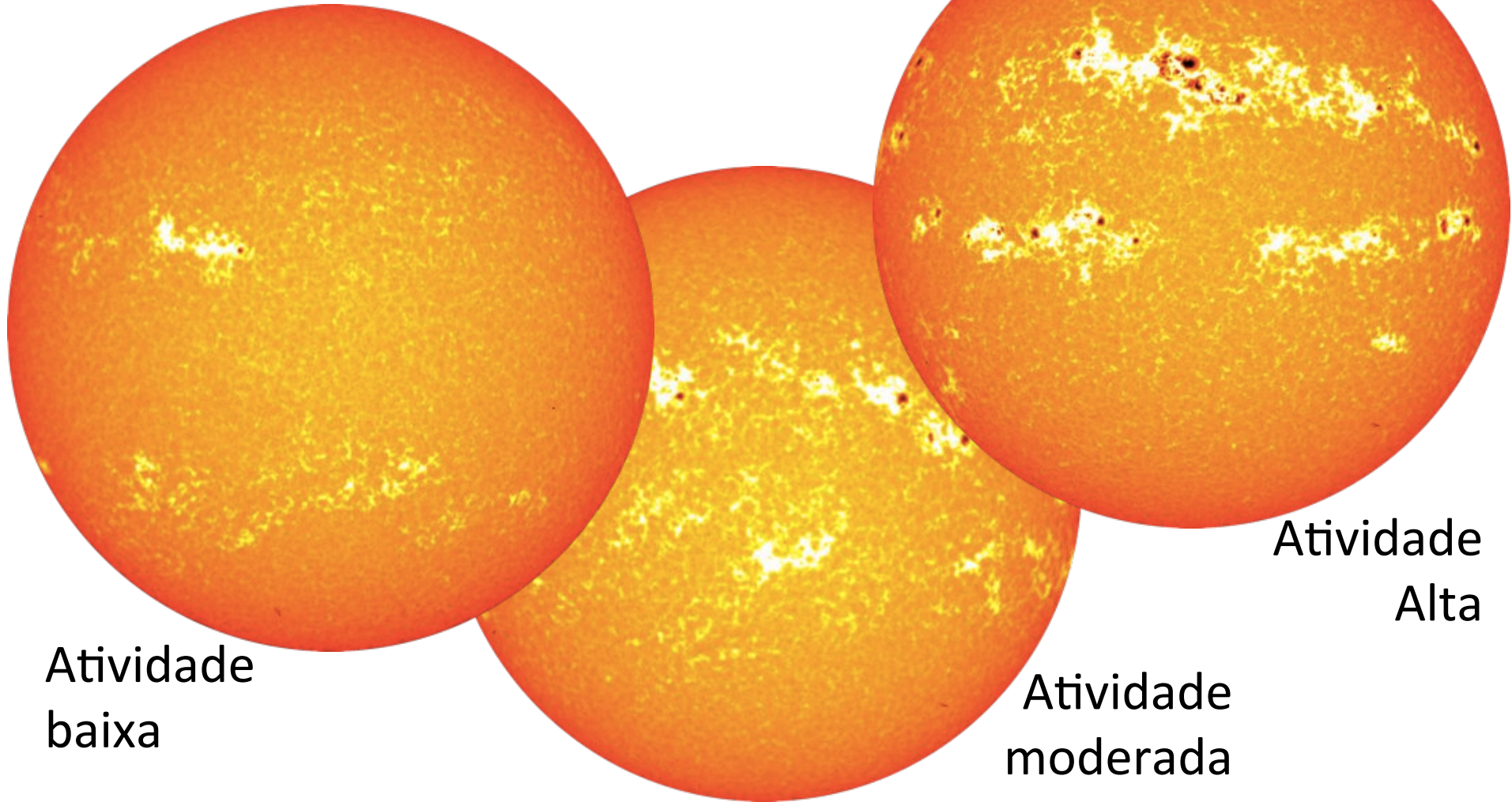


**Sol no mínimo de
atividade: sem manchas**



**Sol no máximo de
atividade: maior número
de manchas**

Sol em $H\alpha$. **Manchas solares:** regiões escuras.
Plages: regiões brilhantes



Atividade
baixa

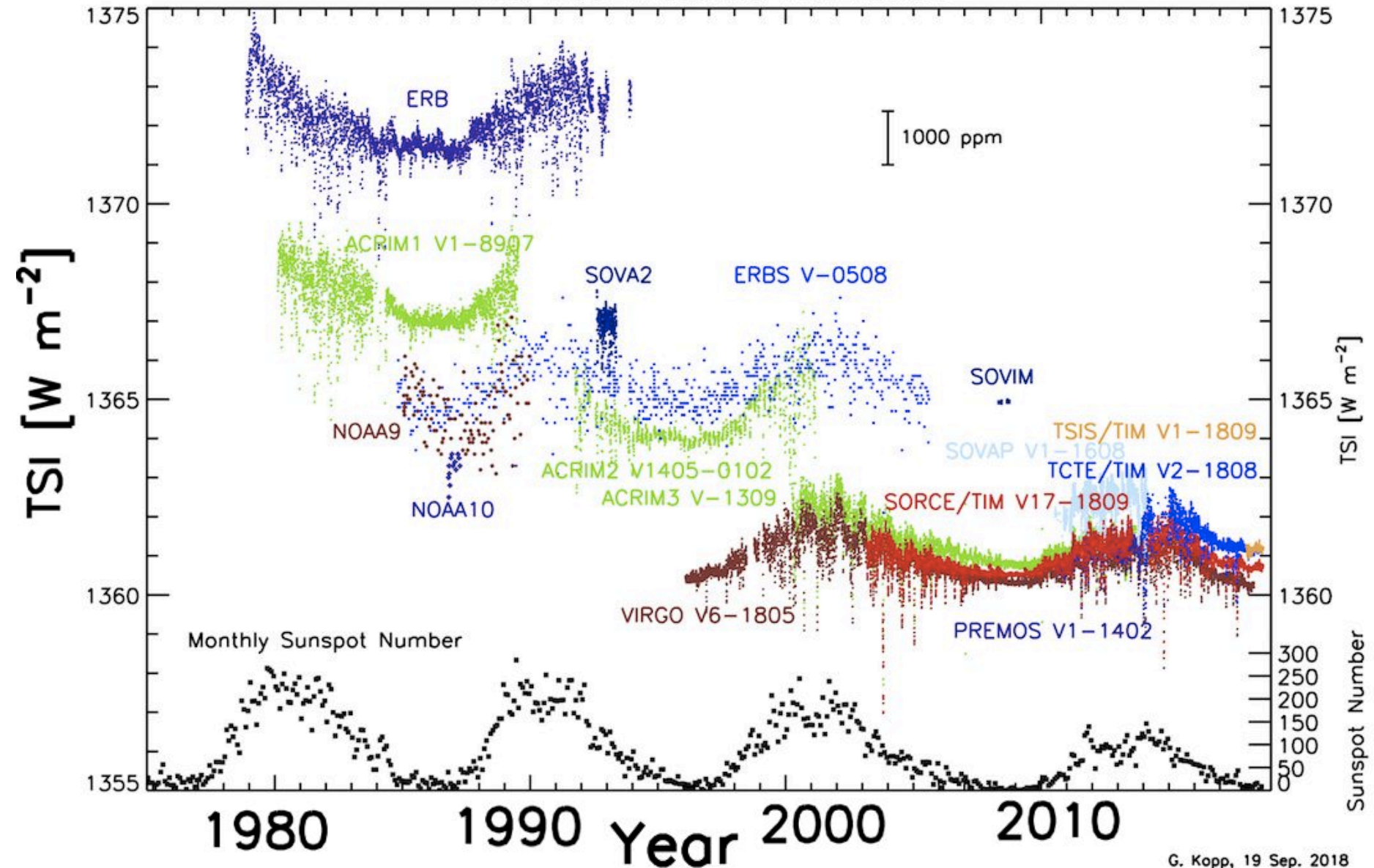
Atividade
moderada

Atividade
Alta

Views of the Sun showing different levels of activity. The color table has been altered to enhance faculae/plage (white regions) which are hotter than sunspots (red-black regions) and whose greater total area contribute to increasing the solar flux reaching the Earth. <https://svs.gsfc.nasa.gov/2644>

Irradiância Solar Total (TSI)

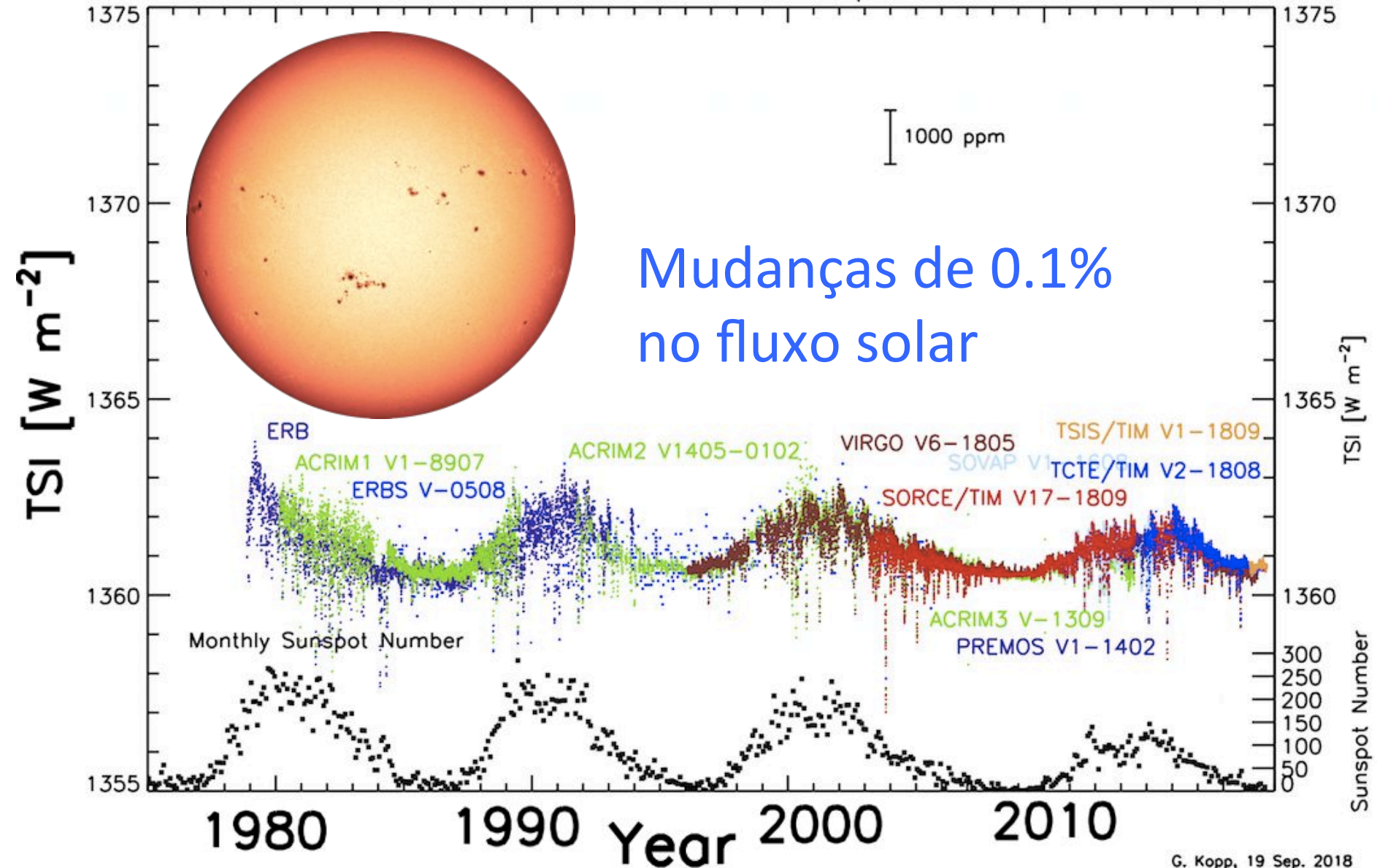
Total Solar Irradiance Data Record



G. Kopp, 19 Sep. 2018

Irradiância Solar Total (TSI)

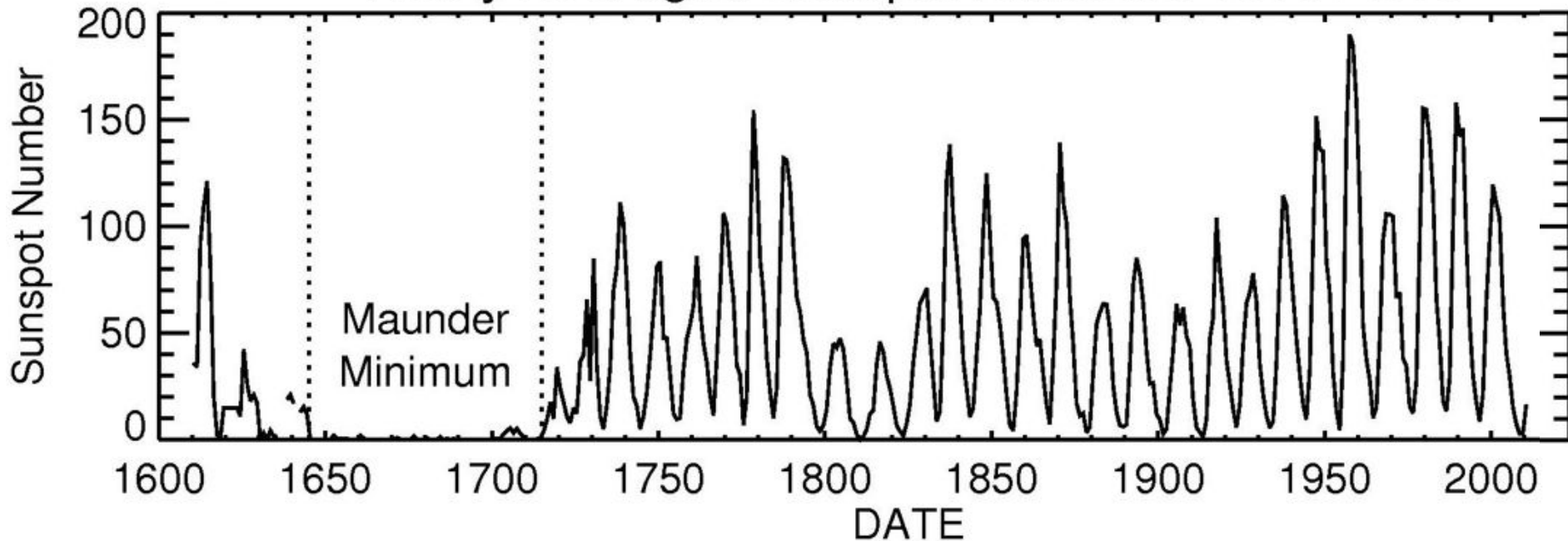
Total Solar Irradiance Composite

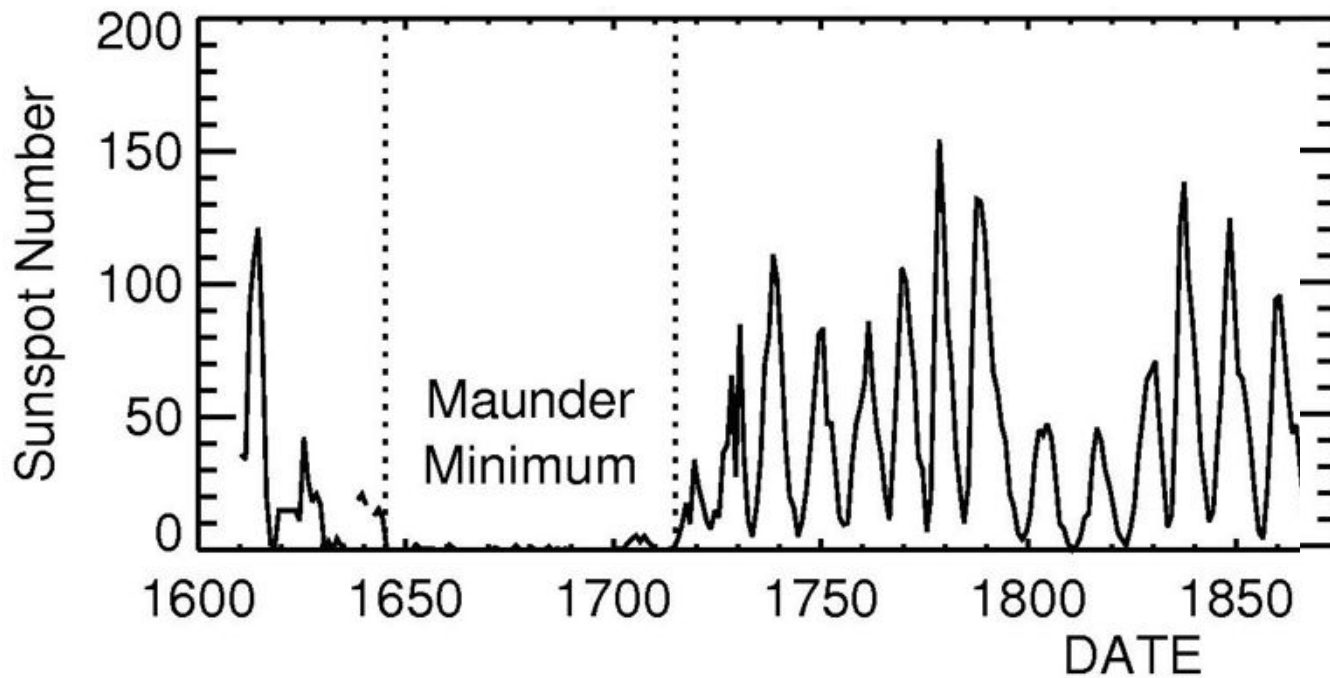


G. Kopp, 19 Sep. 2018

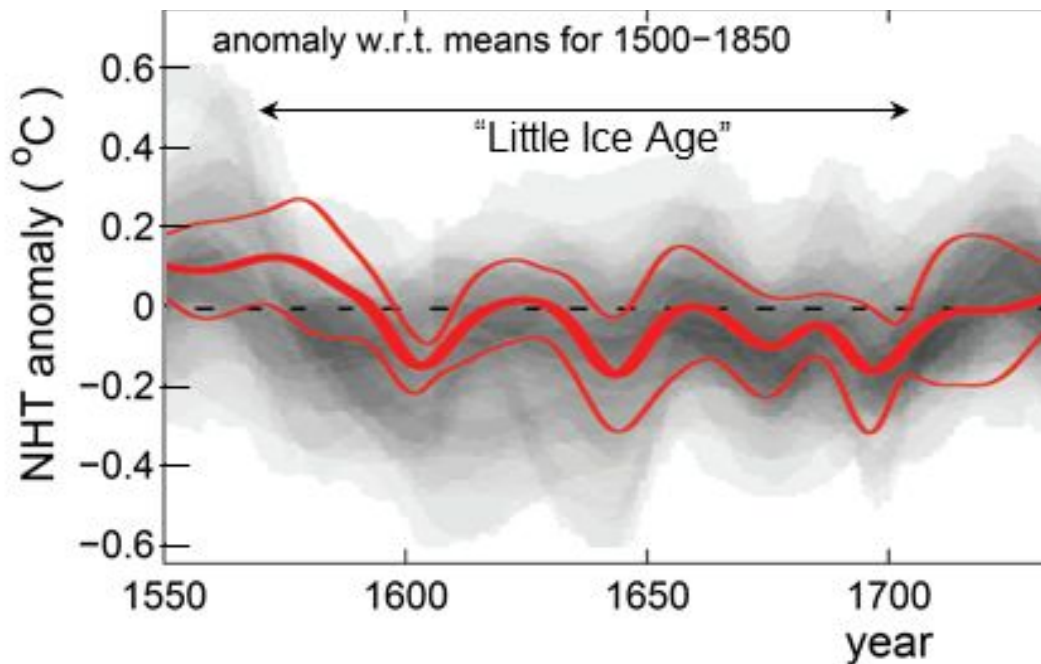
Mínimo de Maunder: entre 1645 e 1715 as manchas solares tornaram-se raras

Yearly Averaged Sunspot Numbers 1610-2010

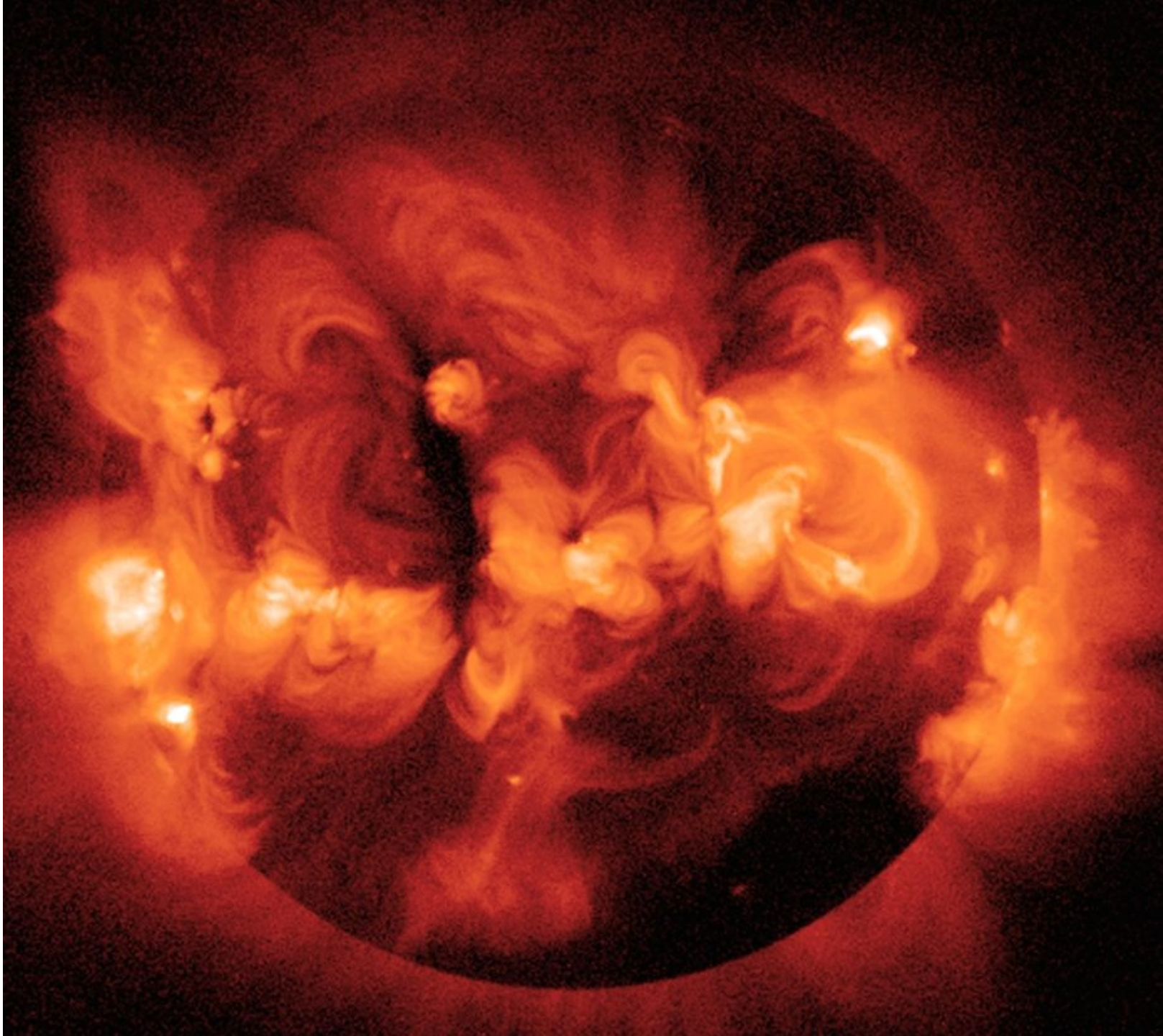




Talvez sem
conexão com
pequena
idade de gelo

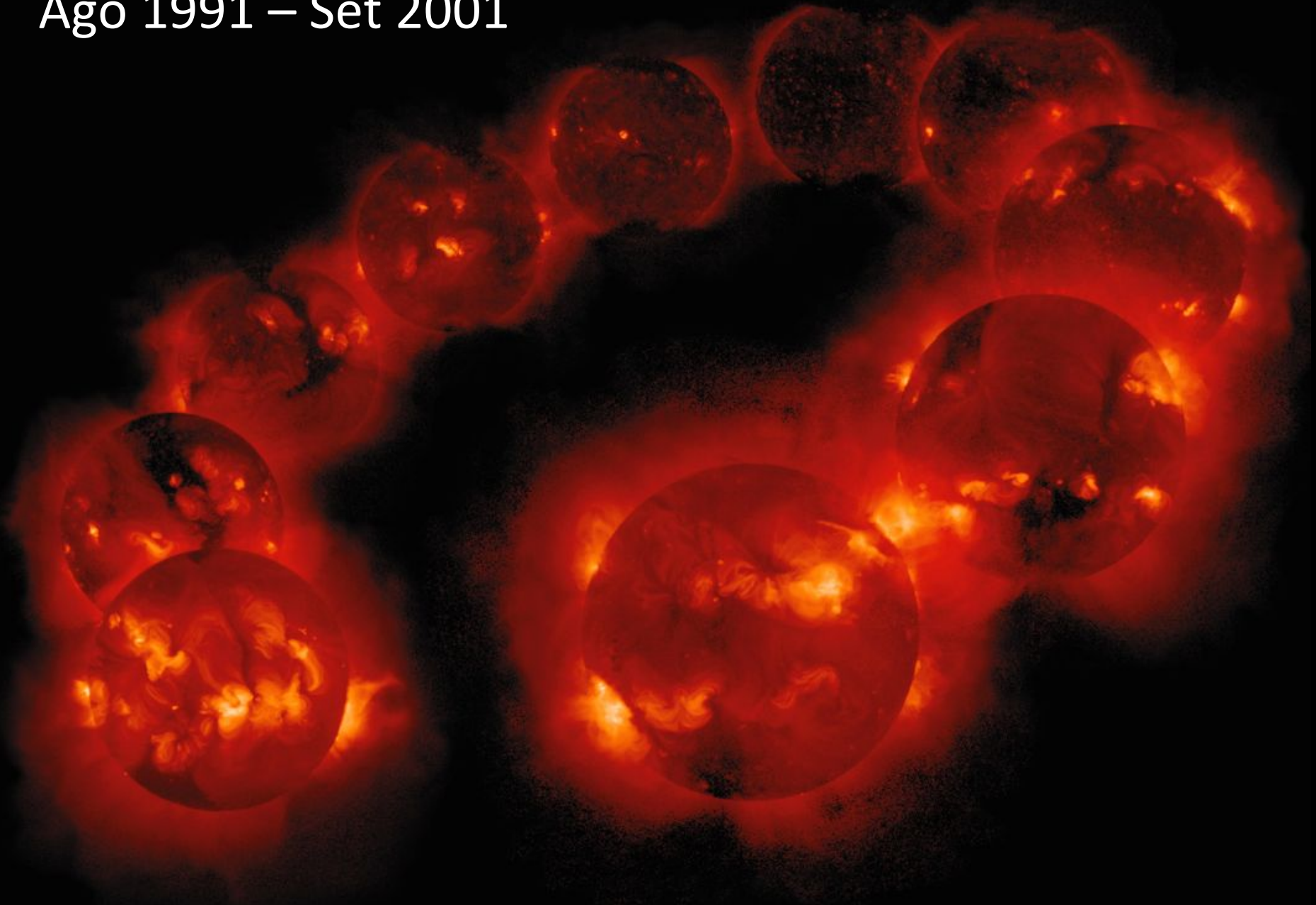


Sol em
raios-X
pelo
Yohkoh
em
1991



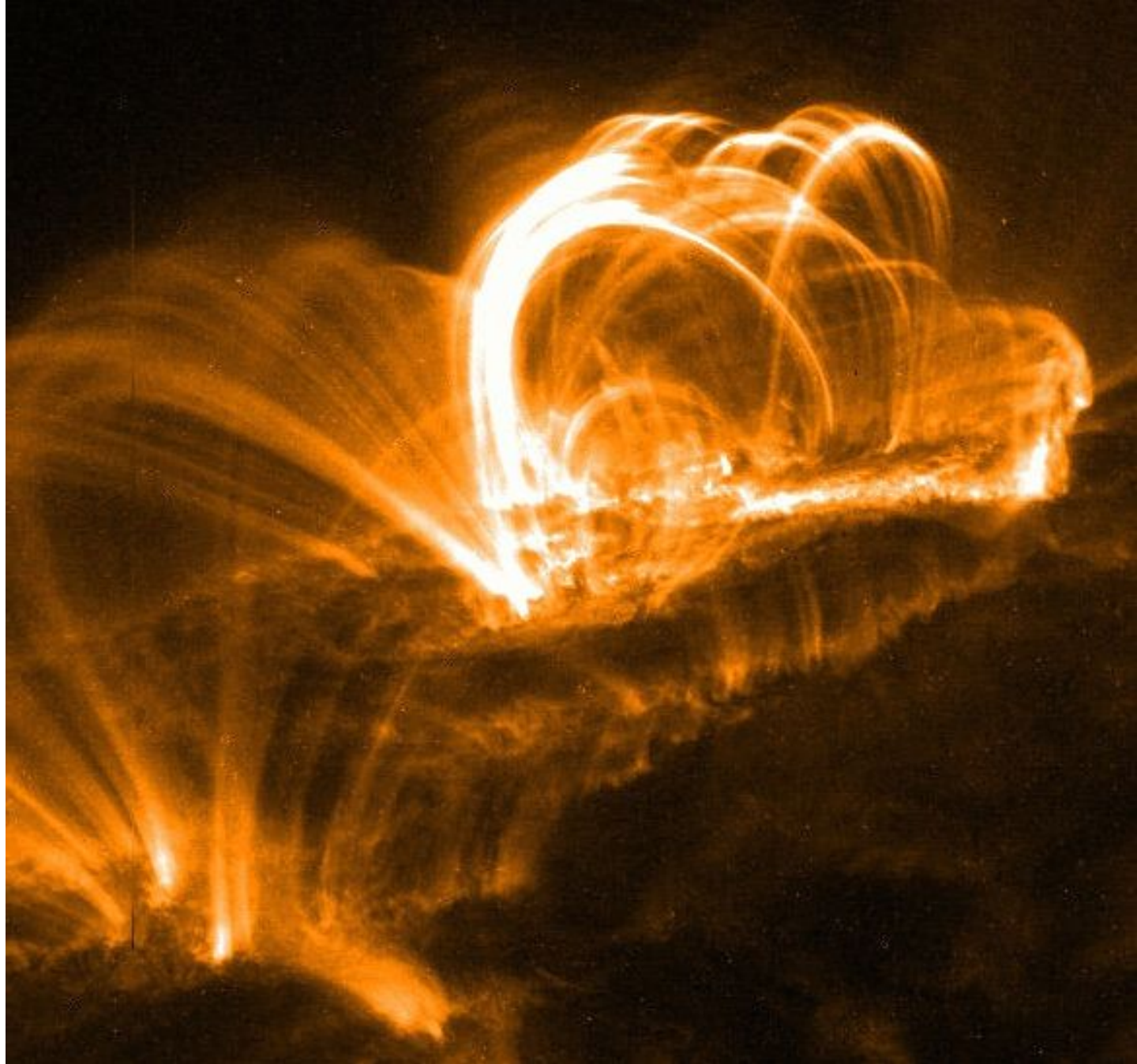
Ciclo de atividade solar em raios-X pelo Yohkoh

Ago 1991 – Set 2001



Solar flare

Image of a typical solar flare from our sun, from September 2005, captured in the X-ray waveband by NASA's TRACE satellite. Note the bright magnetic loops of matter. The twisting and reconnecting of these loops initiate the flare.



Flare solar (erupção solar)

- Energia liberada de 10^{17} - 10^{25} J entre milisegundos a horas.
- Temperatura $\sim 10^7$ K



FIGURE 11.34 (a) A solar flare seen at the limb of the Sun, observed by the Yohkoh Soft X-ray Telescope, March 18, 1999, 16:40 UT. (From the Yohkoh mission of ISAS, Japan. The X-ray telescope

Também são
ejetados raios
cósmicos

Densidade de
energia magnética:

$$u_m = \frac{B^2}{2\mu_0}$$

μ_0 : constante de
permeabilidade
magnética do
vácuo

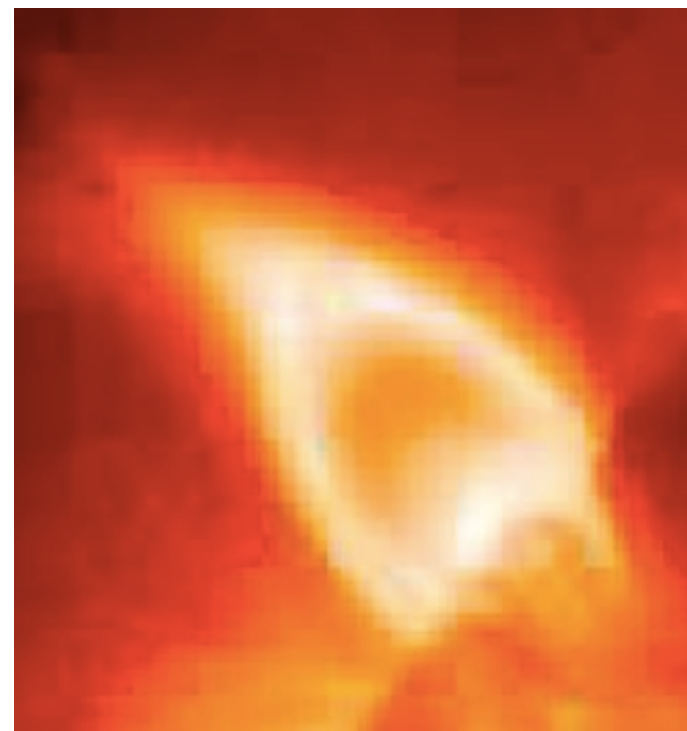
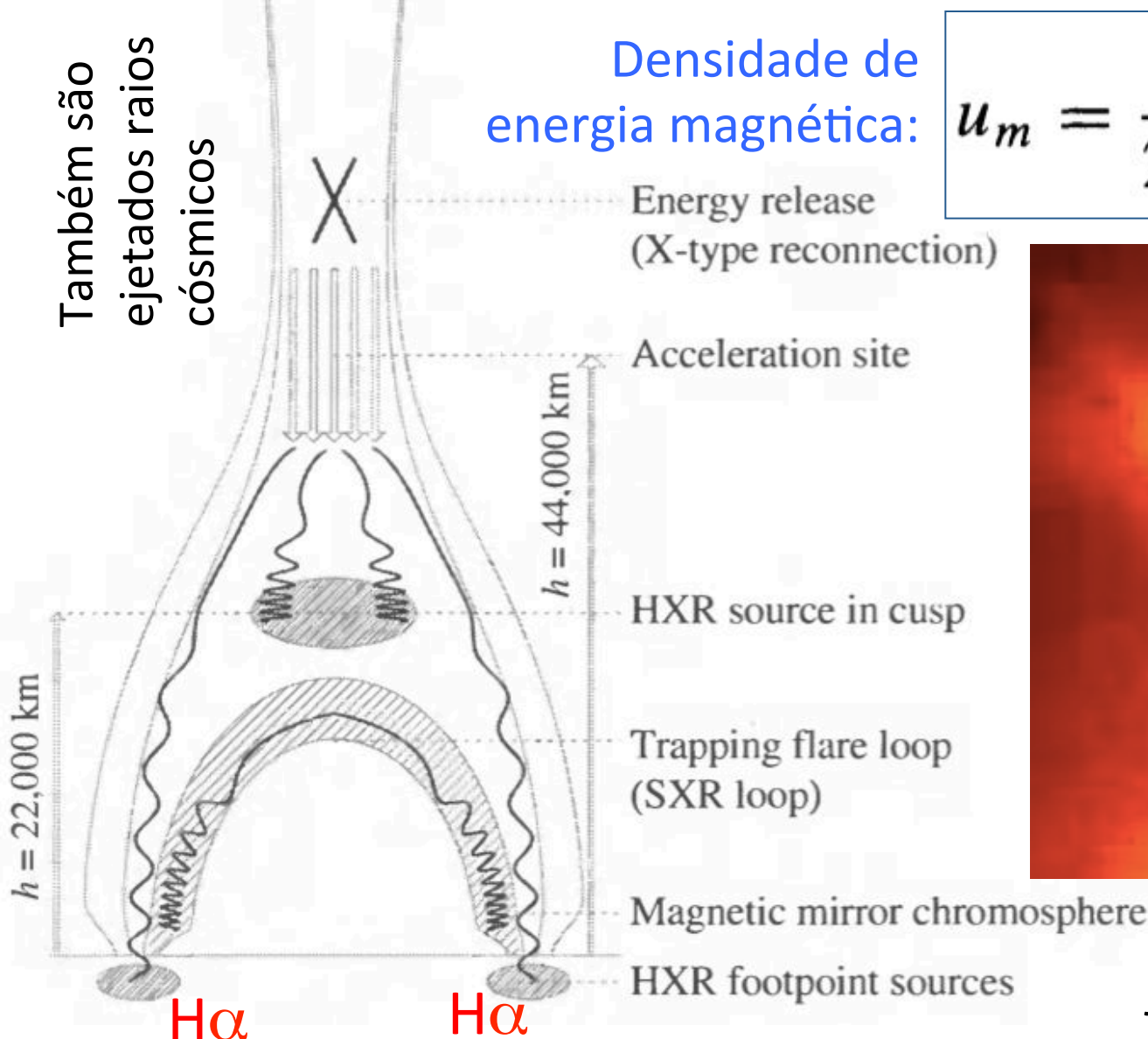
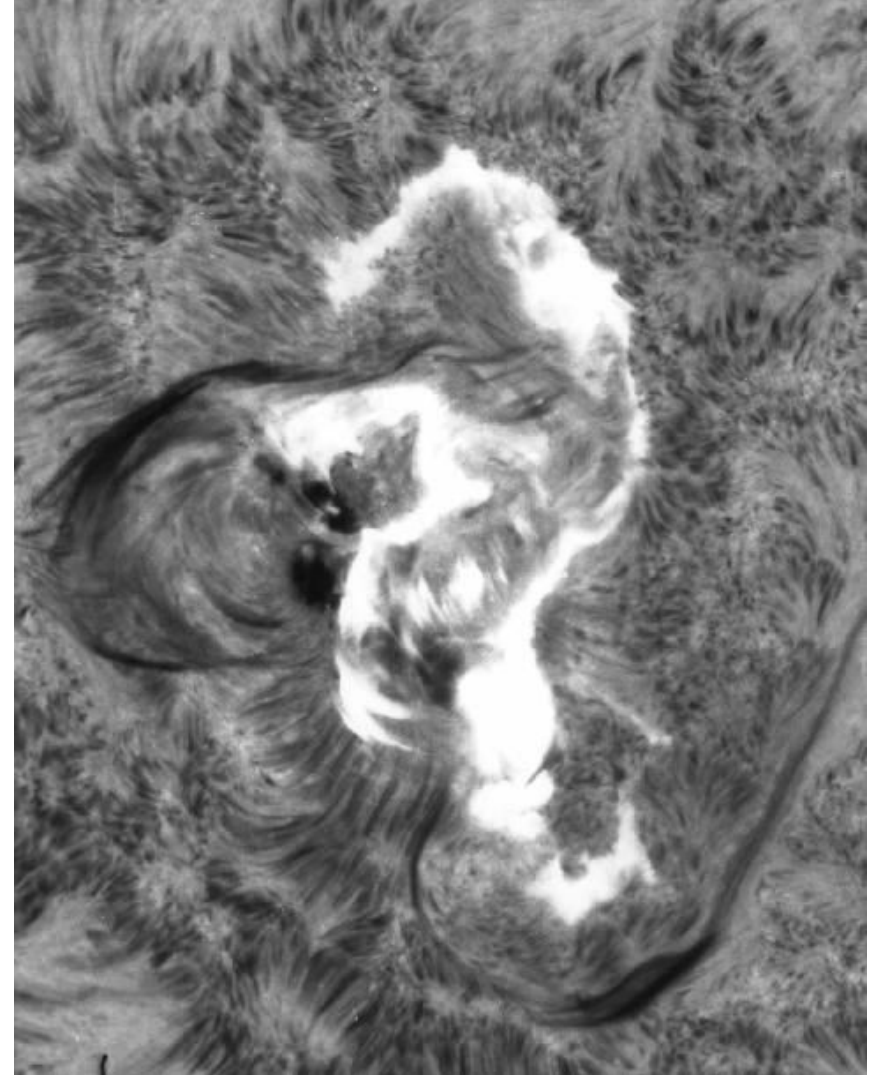
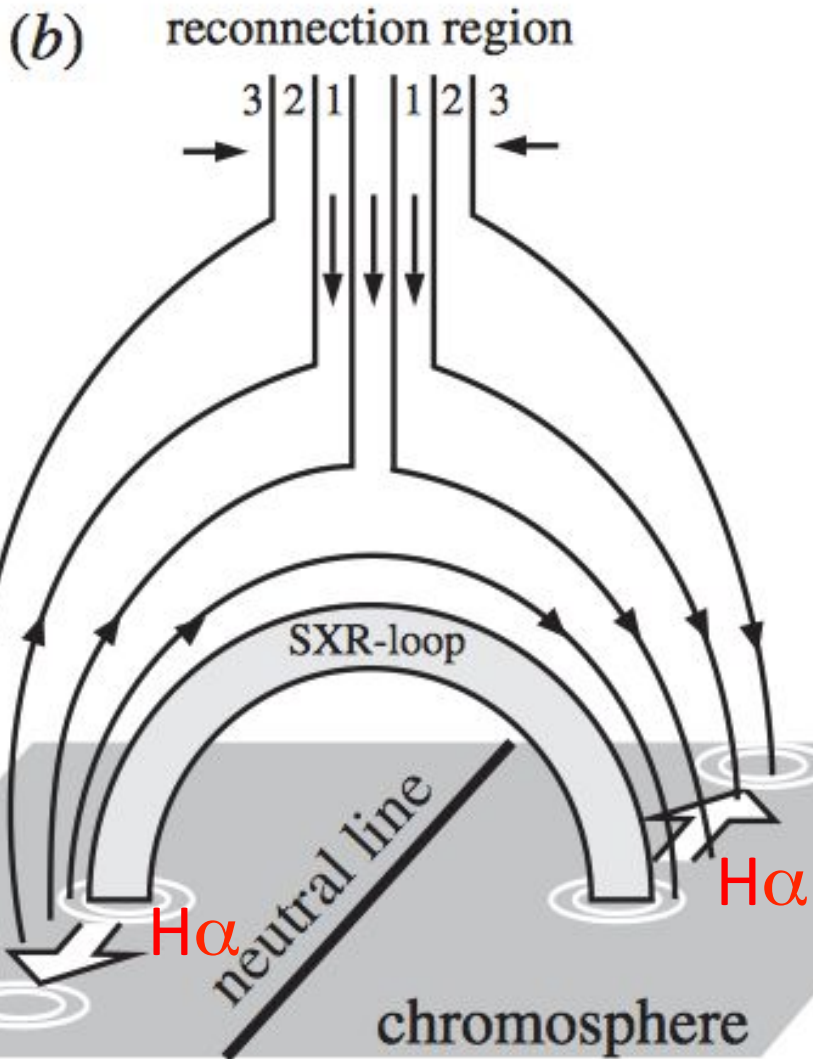


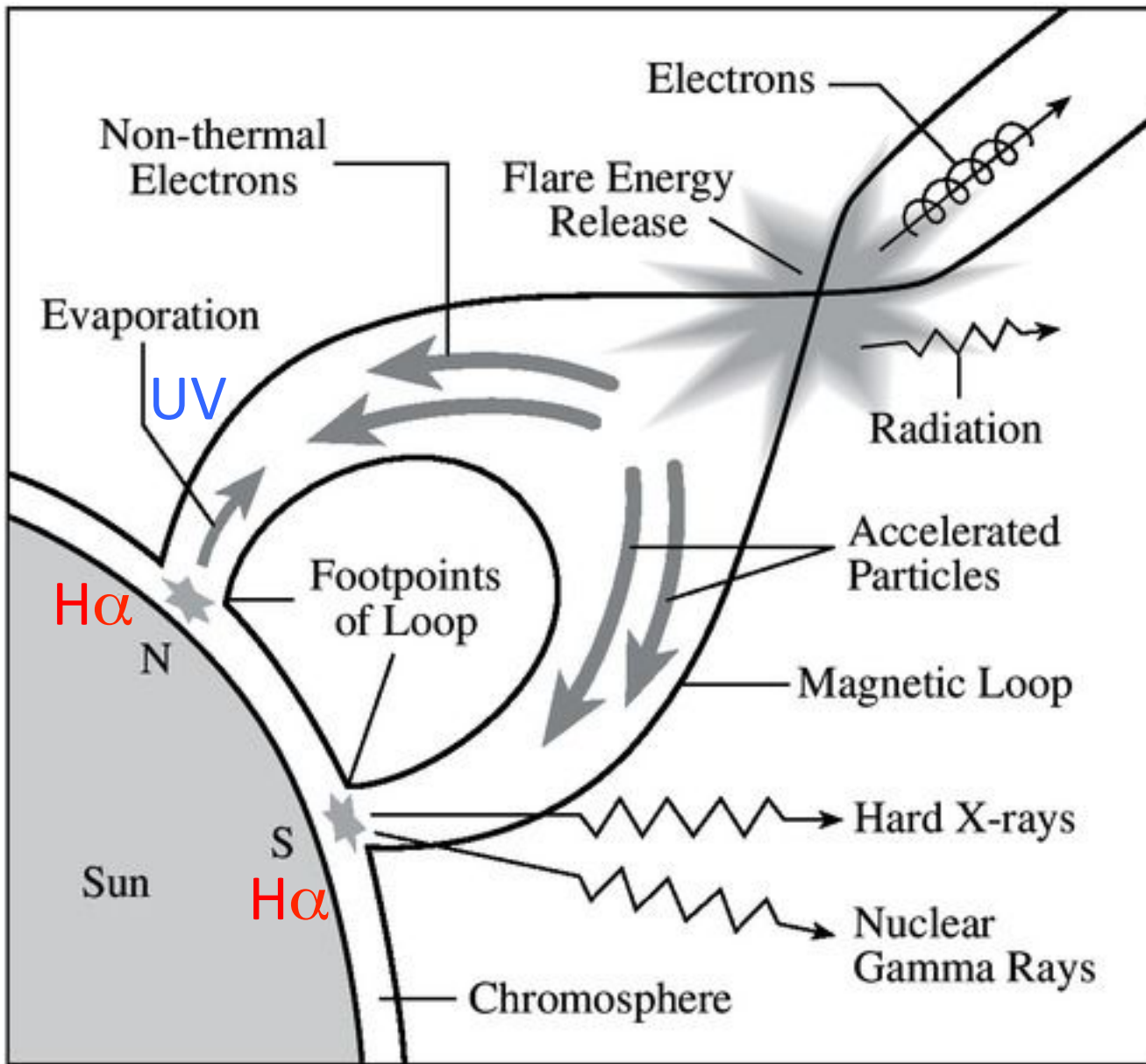
Imagem raios-X de
flare (erupção) solar

FIGURE 11.35 A model of the January 13, 1992, Masuda solar flare. Note the two hard X-ray (HXR) footpoint sources associated with H α flare ribbons [see Fig. 11.34(b)]. Electrons are accelerated downward along the magnetic field lines until they collide with the chromosphere. The soft X-ray (SXR) loop may be compared to Fig. 11.34(a). (Figure adapted from Aschwanden, et al., *Ap. J.*, 464, 985, 1996.)



The great 'Seahorse Flare' of August 7th, 1972: This image in H-alpha shows the two-ribbon structure late in the event, with bright H-alpha loops connecting the ribbons.

Fig. 3b, Solar flares and energetic particles
NICOLE VILMER, *Phil. Trans. R. Soc. A* (2012)
370, 3241

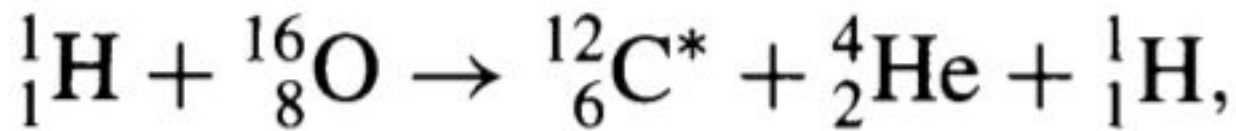


Radio:
synchrotron

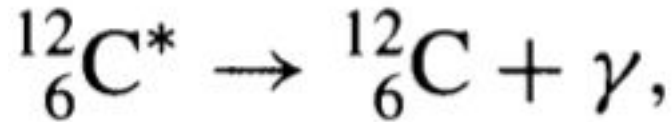
Soft X-rays: altas
temperaturas

Hard X-ray:
Bremsstrahlung

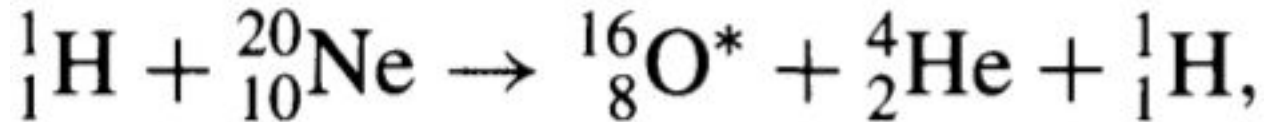
Gamma rays:
reações nucleares



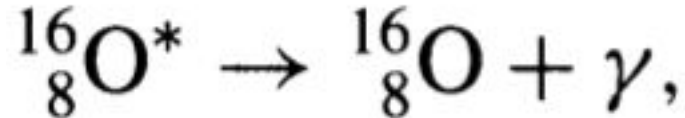
where C^* represents a carbon nucleus in an excited state, followed by the de-excitation reaction



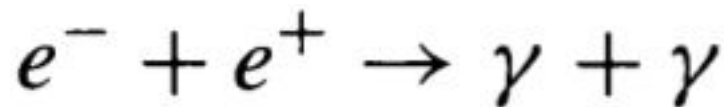
with $E_\gamma = 4.438$ MeV, or



followed by the de-excitation reaction



with $E_\gamma = 6.129$ MeV. Other examples of reactions produced by flares on the Sun's surface include electron-positron annihilation,



where $E_\gamma = 0.511$ MeV, and the production of deuterium by




where $E_\gamma = 2.223$ MeV.

An **eruptive prominence** in extreme UV light on March 30, 2010. Credit: NASA/SDO.

A prominence (also known as a filament when viewed against the solar disk) is a large, bright feature extending outward from the Sun's surface. Prominences are anchored to the Sun's photosphere, and extend outwards into the Sun's corona. A prominence forms over timescales of ~ 1 day, and stable prominences may persist for months. The red-glowing looped material is plasma, flowing along a tangled & twisted structure of magnetic fields generated by the sun's internal dynamo. An erupting prominence occurs when such a structure becomes unstable and bursts outward, releasing the plasma.

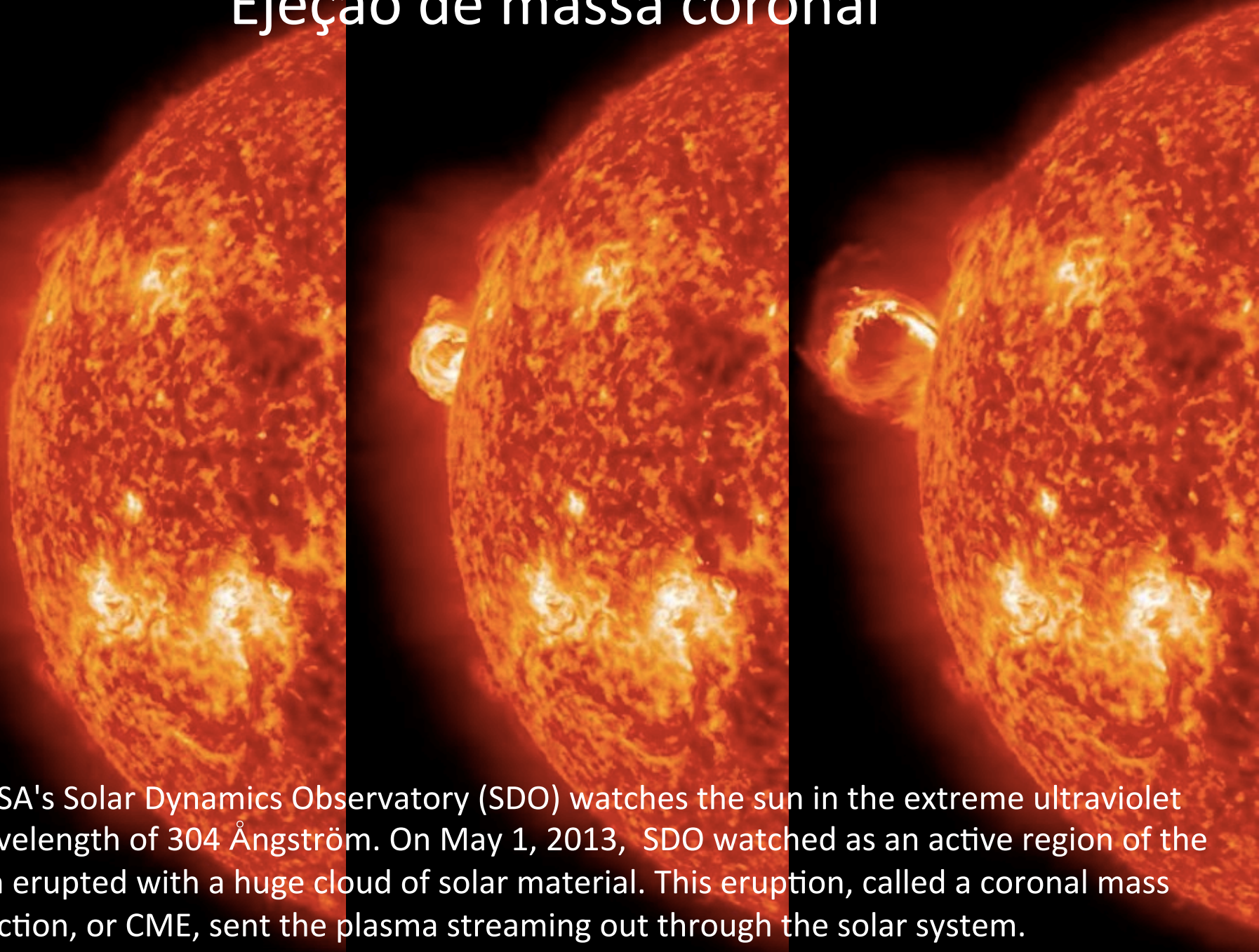
Proeminência solar

Approx. size of Earth → 



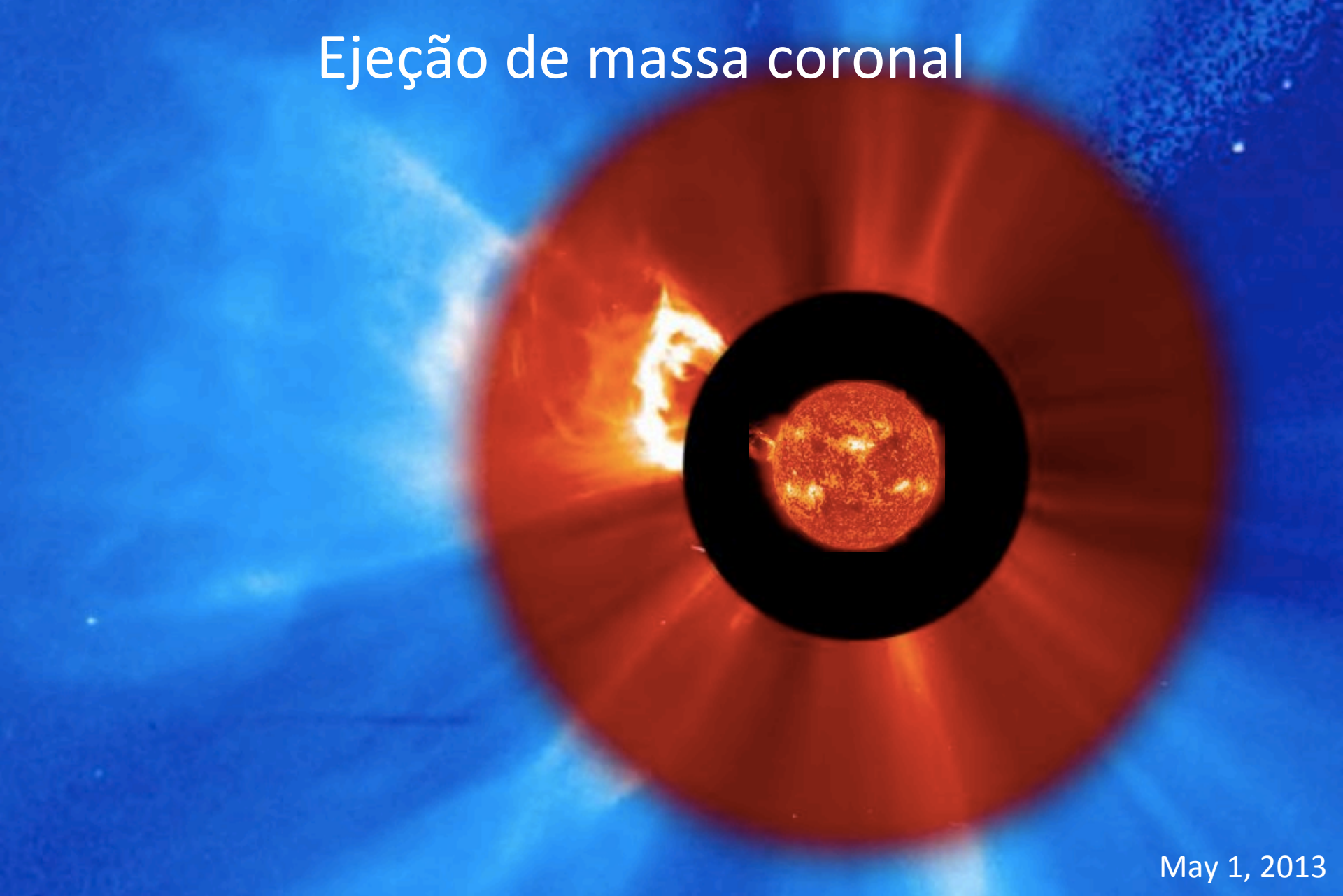
<https://www.nasa.gov/content/goddard/what-is-a-solar-prominence>

Ejeção de massa coronal



NASA's Solar Dynamics Observatory (SDO) watches the sun in the extreme ultraviolet wavelength of 304 Ångström. On May 1, 2013, SDO watched as an active region of the sun erupted with a huge cloud of solar material. This eruption, called a coronal mass ejection, or CME, sent the plasma streaming out through the solar system.

Ejeção de massa coronal



May 1, 2013

Besides the SDO images, the CME was also observed by SOHO using 2 coronagraphs where the bright sun is blocked by a disk so it does not overpower the fainter corona.

Máximo do ciclo de atividade:

~ 3,5 por dia

Mínimo: aprox.
1 cada 5 dias.

5×10^{12} kg a
 5×10^{13} kg

$v \sim 400$ km/s a
 1000 km/s

Com *flares*: 40%

Com proeminência solar eruptiva: 70%

Ejeção de massa coronal



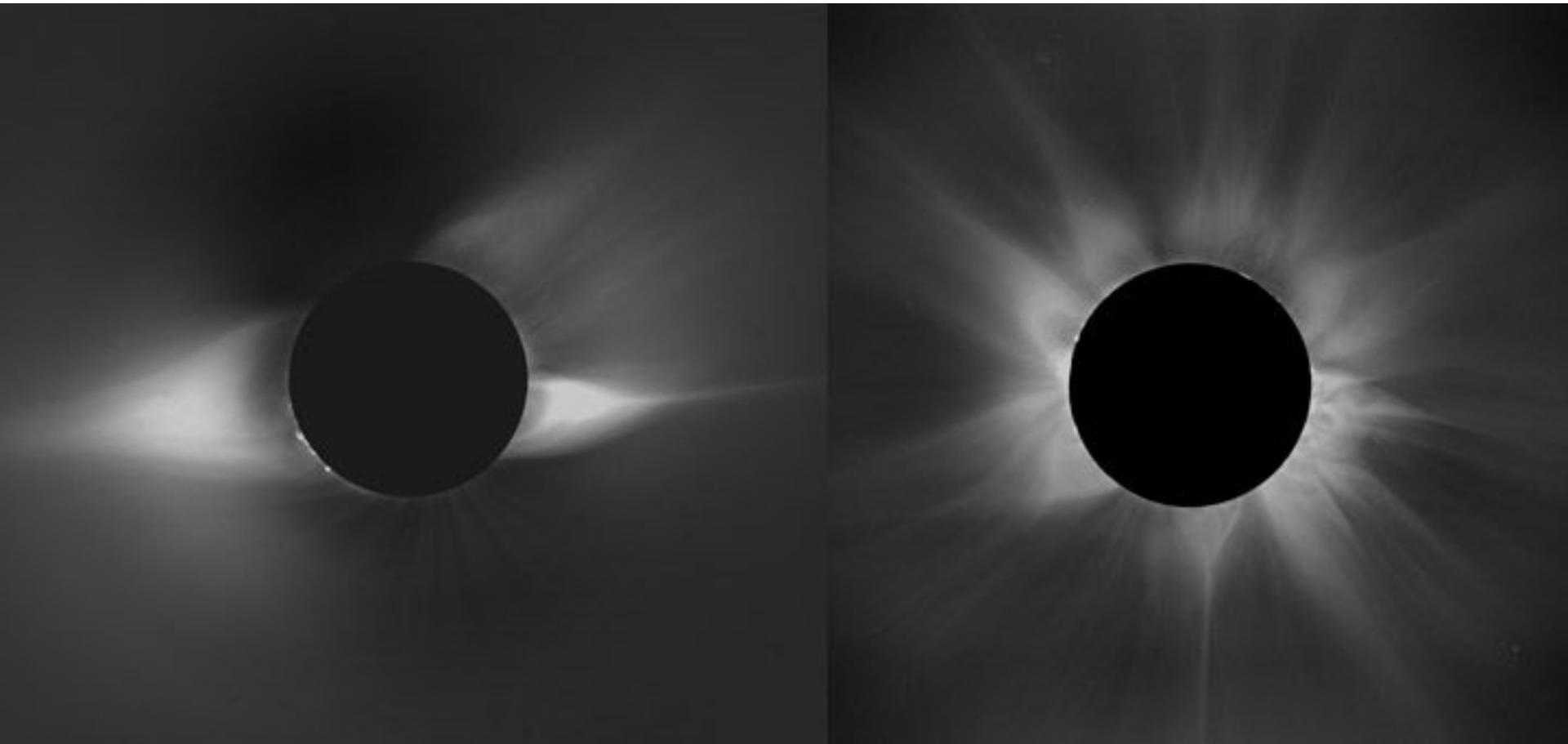
Coroa solar durante eclipse

1994 (mínimo de atividade)

Mais extendida no equador,
consistente com campo dipolar

1980 (máximo de atividade)

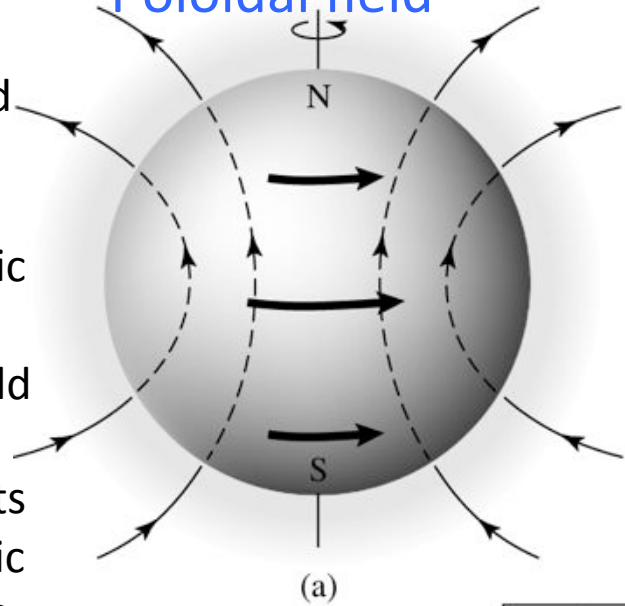
Coroa é mais complexa



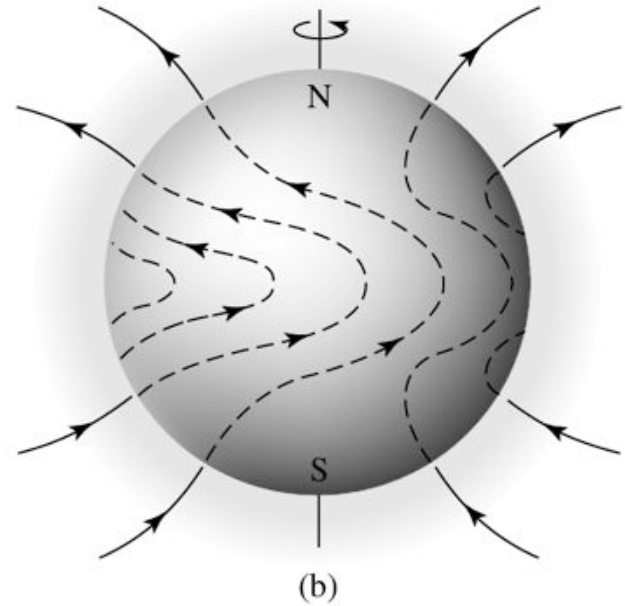
The magnetic dynamo model of the solar cycle.

(a) The solar magnetic field is initially poloidal (simple dipole). (b) Differential rotation drags the magnetic field lines around the Sun, converting the poloidal field into a toroidal field. (c) Turbulent convection twists the field lines into magnetic ropes, causing them to rise as sunspots, the polarity of the lead spots corresponds to the original polarity of the poloidal field. (d) As the cycle progresses, successive sunspot groups migrate toward the equator where magnetic field reconnection reestablishes the poloidal field, but with the original polarity reversed.

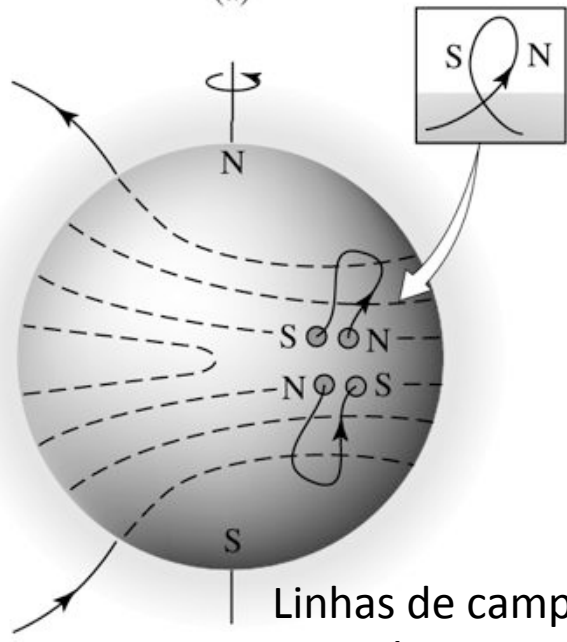
Poloidal field



(a)



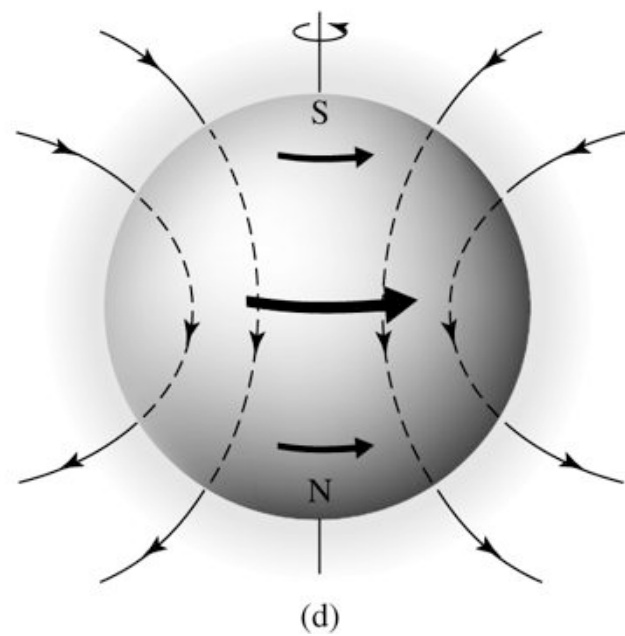
(b)



(c)

Linhas de campo magnético mais enroladas

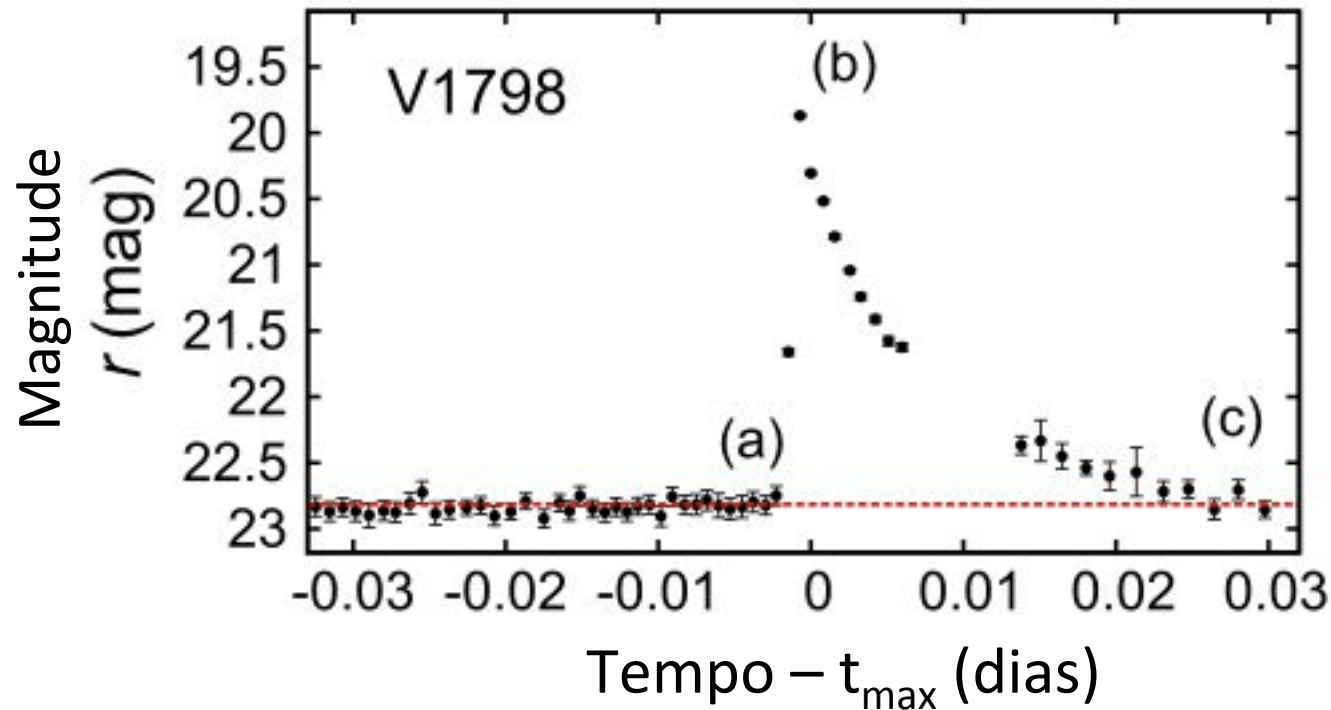
Toroidal field



(d)

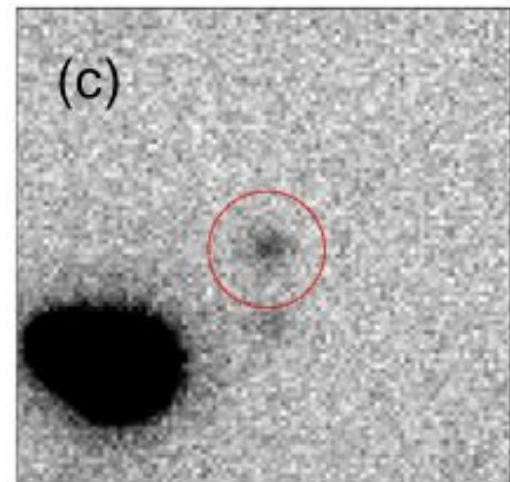
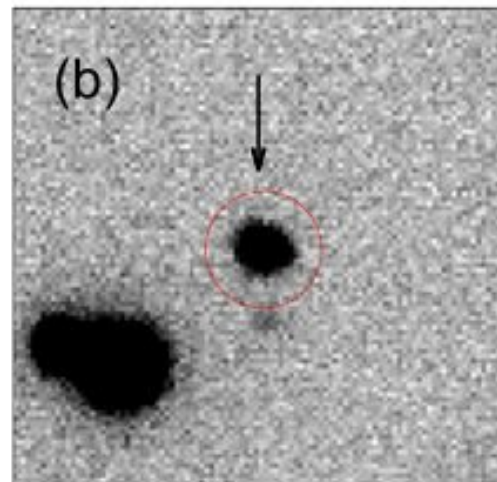
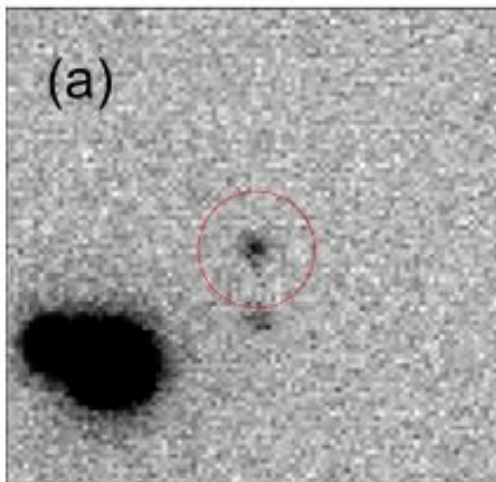
Poloidal field

Estrelas “flare” (geralmente estrelas M)



Anã M no
aglomerado
aberto M37

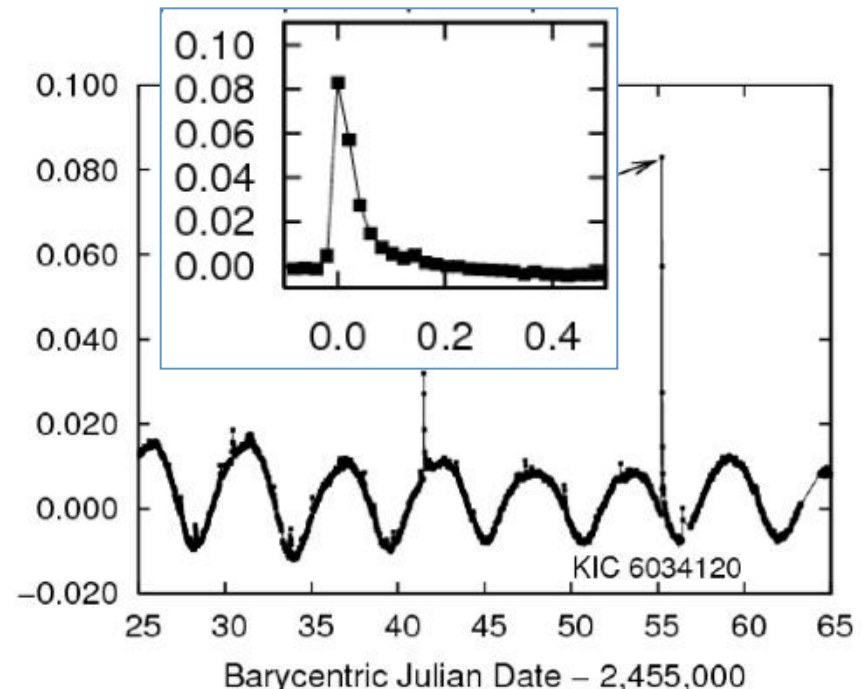
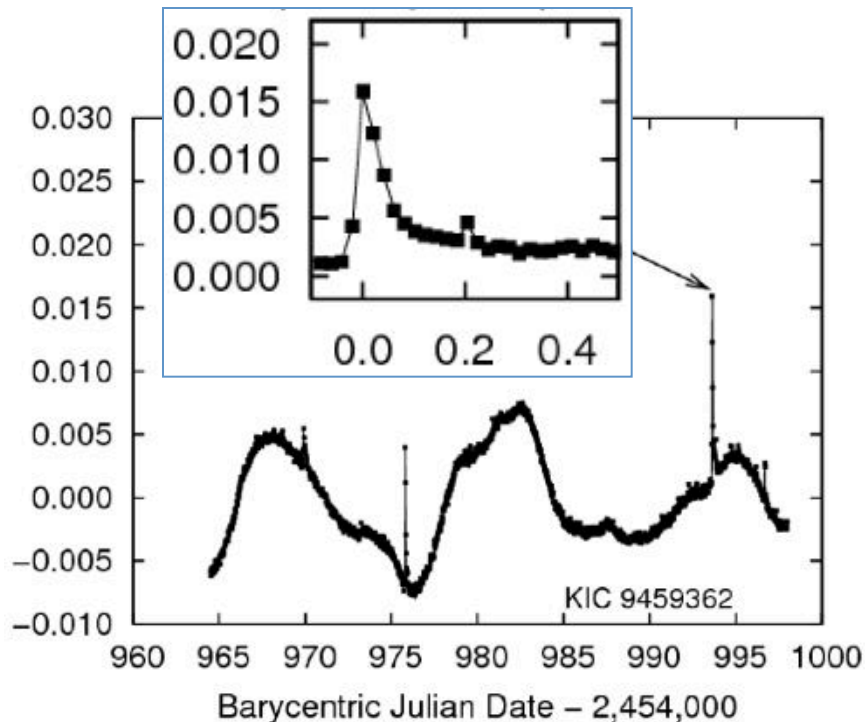
Chang et al. 2015,
ApJ 814, 35



Superflares on solar-type stars

Hiroyuki Maehara, Takuya Shibayama, Shota Notsu, Yuta Notsu, Takashi Nagao, Satoshi Kusaba, Satoshi Honda, Daisaku Nogami & Kazunari Shibata

14 flares on 10 Sun-like stars (T_{eff} : 5600-6000; $P > 10$ days)
 Amplitude: 0.1-10%; Duration: ~ 0.1 days
 Total bolometric energy of superflares: 10^{33} - 10^{36} ergs
 10-10,000 times larger than the largest solar flares (10^{32} ergs)



Ciclo de atividade na estrela BD+26730

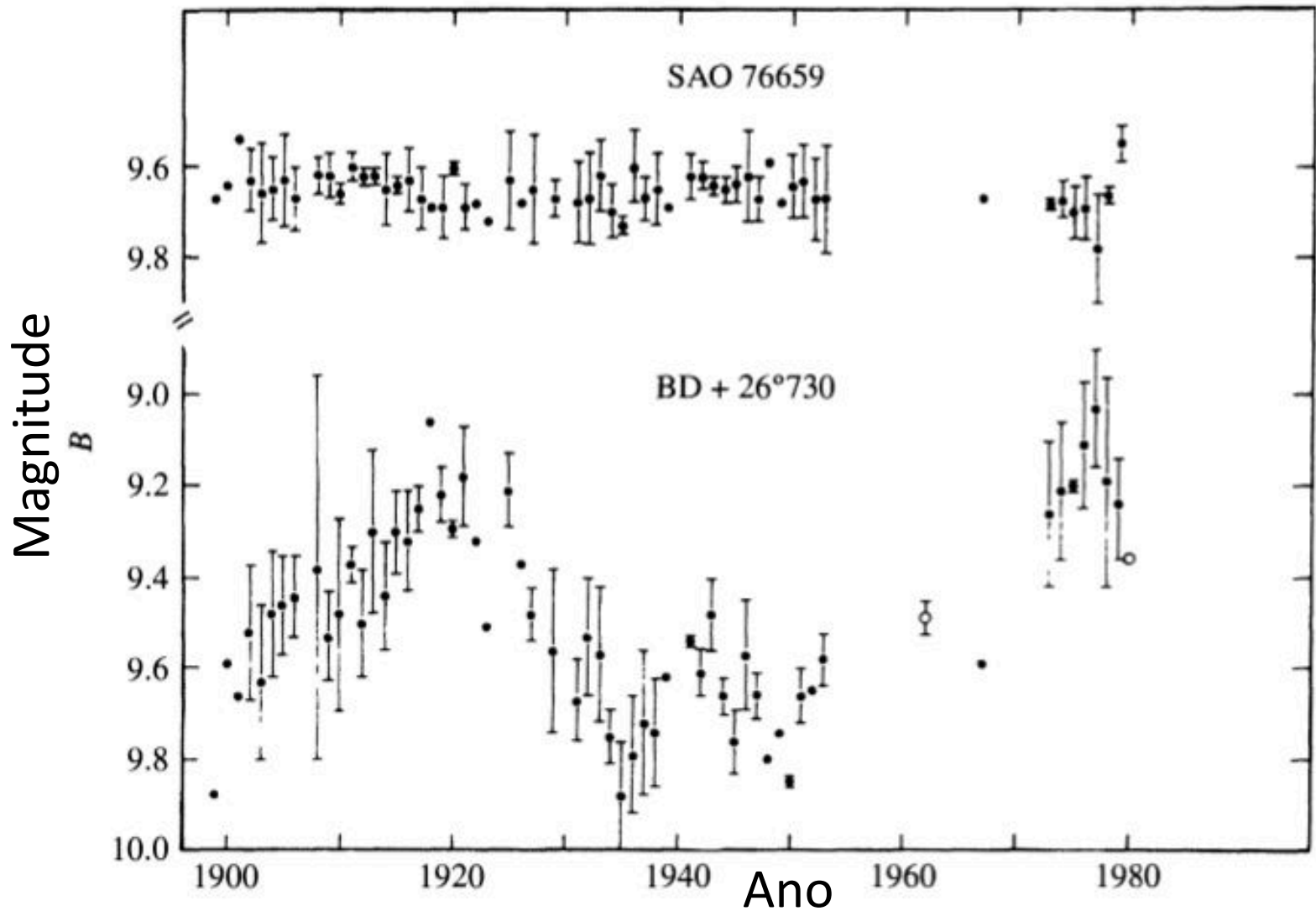
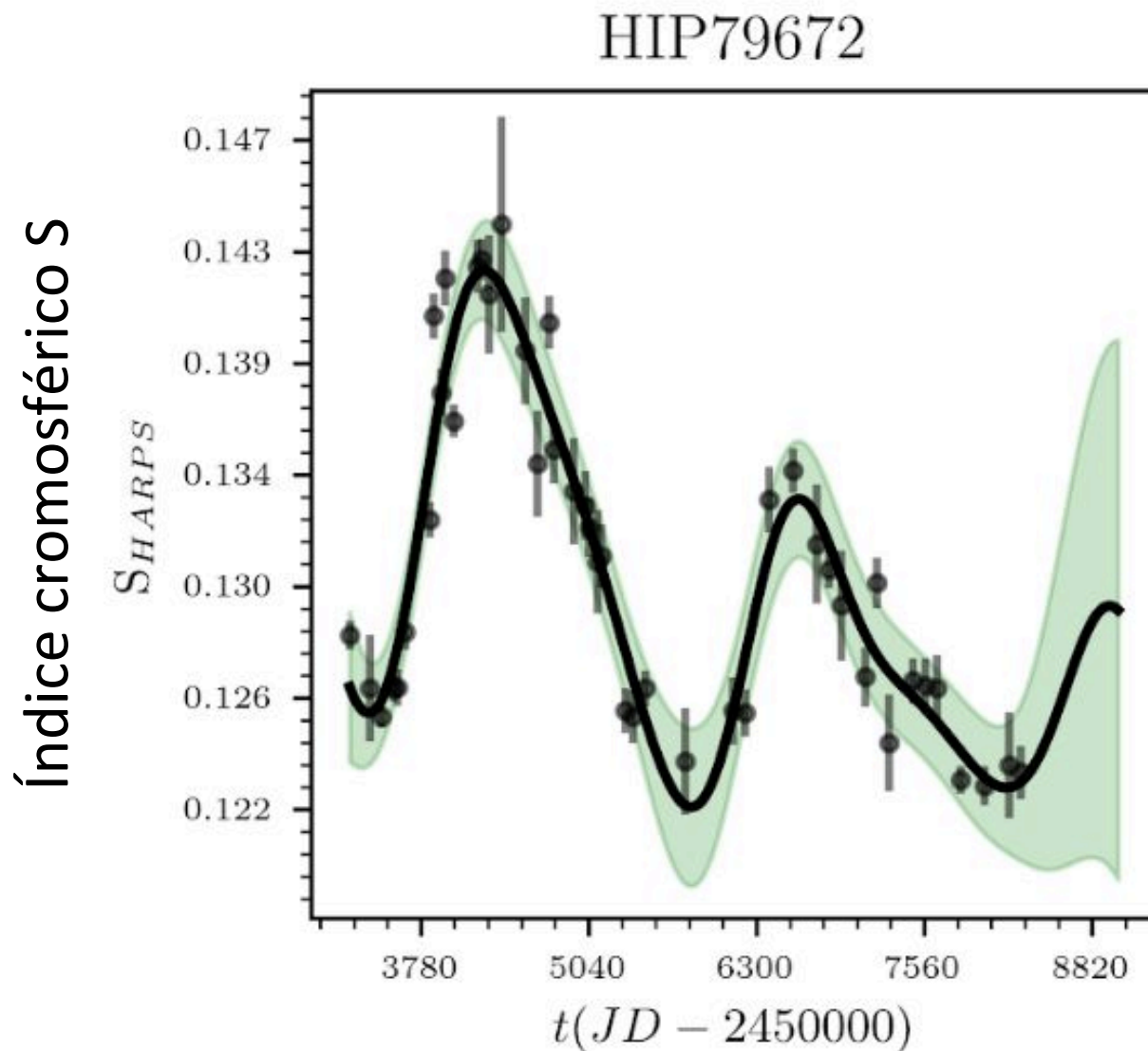
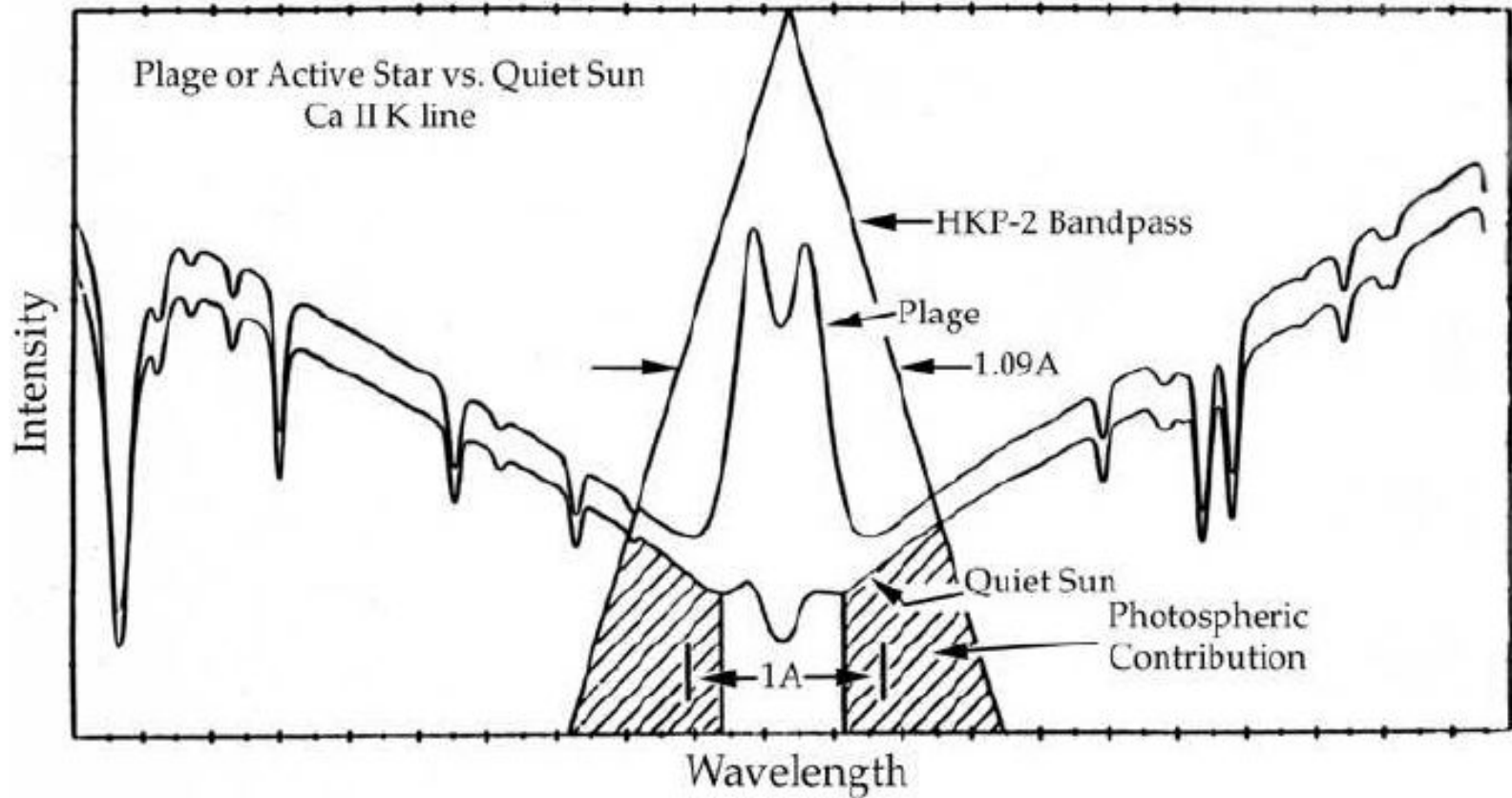


FIGURE 11.39 The light curve of BD + 26°730, a BY Dra star. SAO 76659 is a nearby reference star. (Figure from Hartmann et al., *Ap. J.*, 249, 662, 1981.)

Em estrelas como o Sol (HD 146233 = HIP 79672), as variações do ciclo de atividade podem ser estudadas usando o índice cromosférico S



Linha de absorção fotosférica e emissão cromosférica (no *plage*) da linha K do Ca II

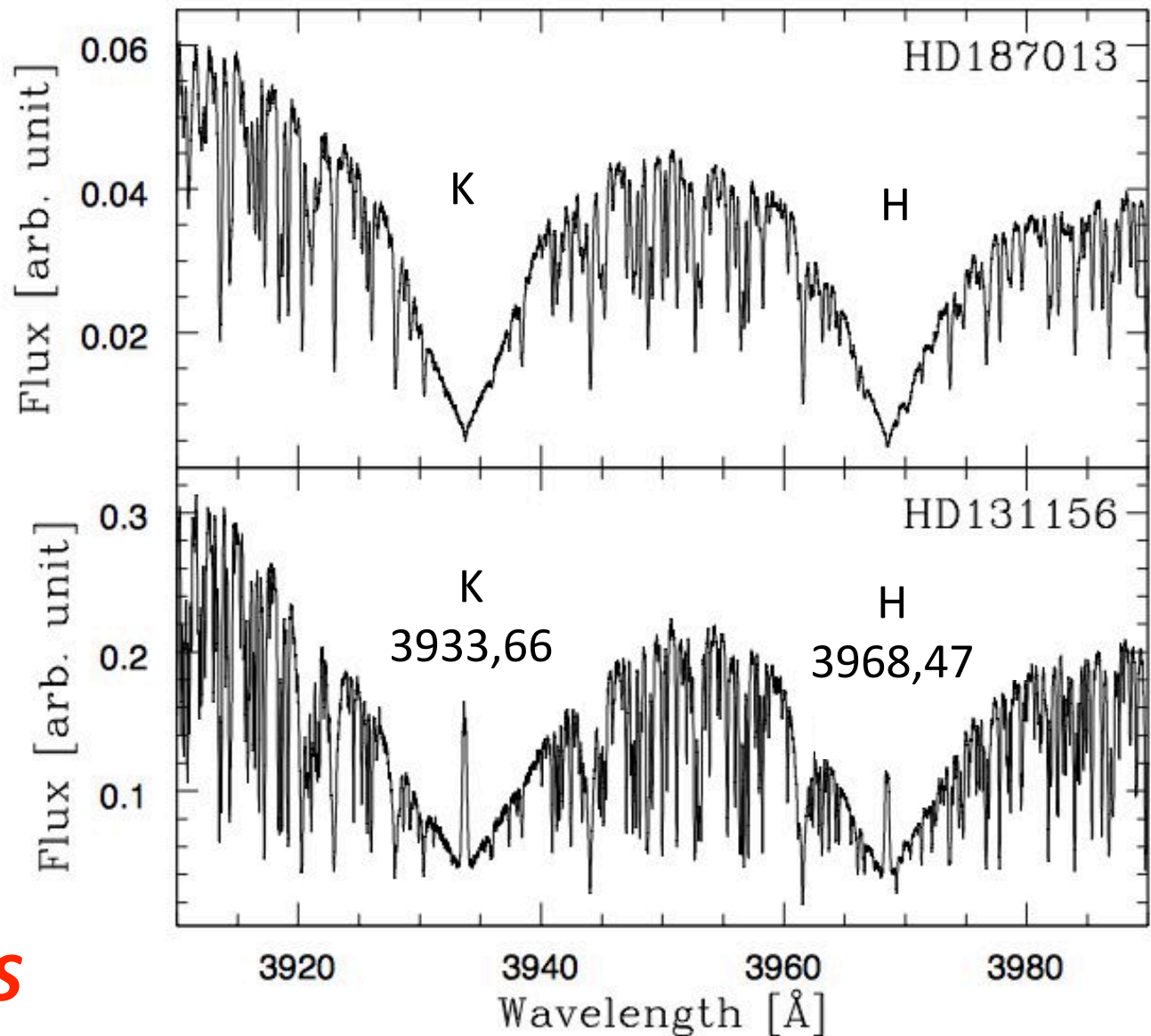


Plage: emissão brilhante na cromosfera

Imagem do Sol em H α

Estrelas ativas apresentam **emissão cromosférica** no centro das linhas H e K do CaII.

Medida da emissão nas linhas H e K → **índice cromosférico S**

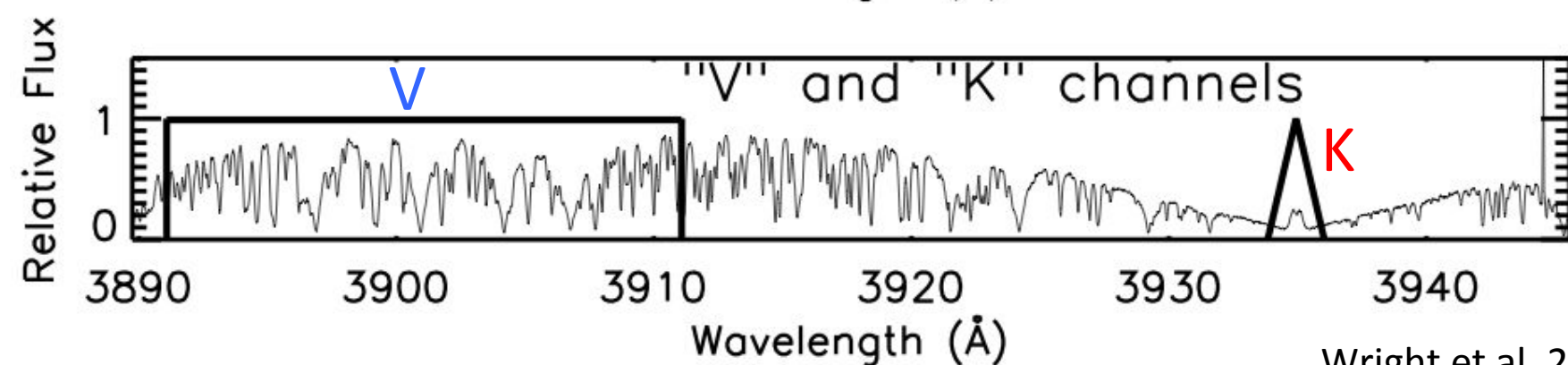
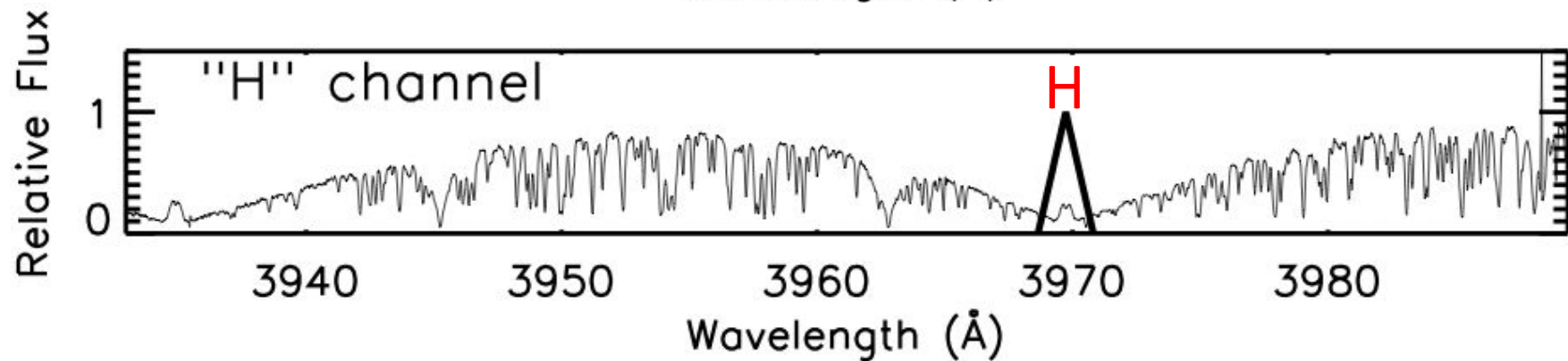
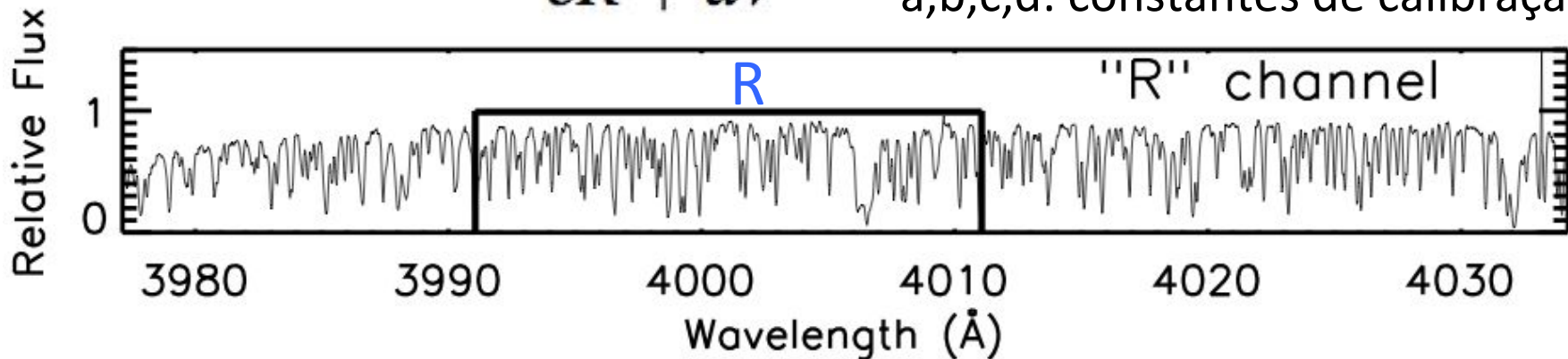


Boisse et al.
2010 A&A 523,
A88

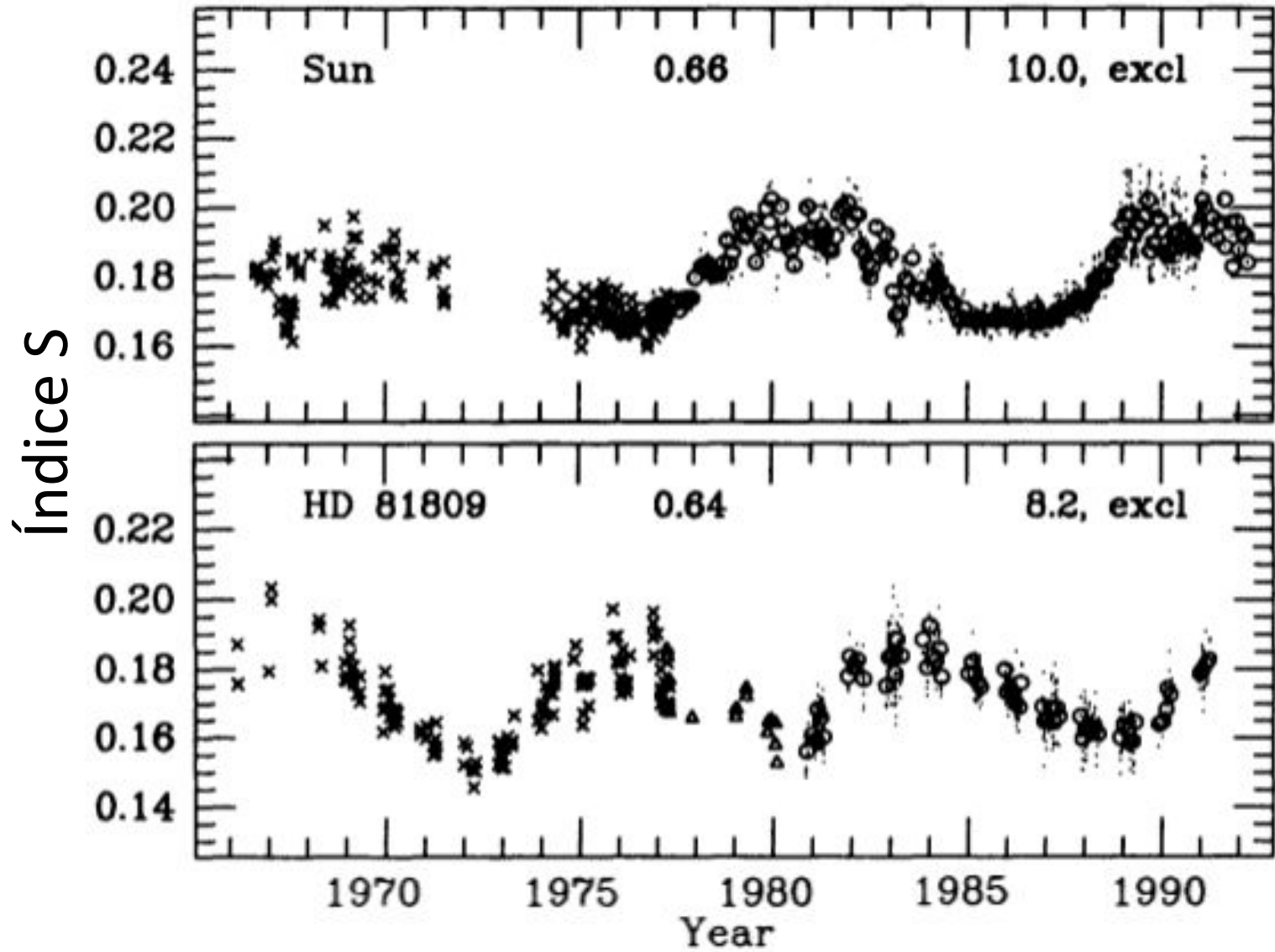
Fig.C.1. Two SOPHIE spectra of the region of the CaII H and K lines between 3900 and 4000 Å. *Bottom:* Active star. *Top:* Non active star.

Índice S:
$$S = \frac{aH + bK}{cR + dV}$$

H, K: fluxo nas bandas das linhas
R, V: fluxo nas bandas de contínuo
a,b,c,d: constantes de calibração

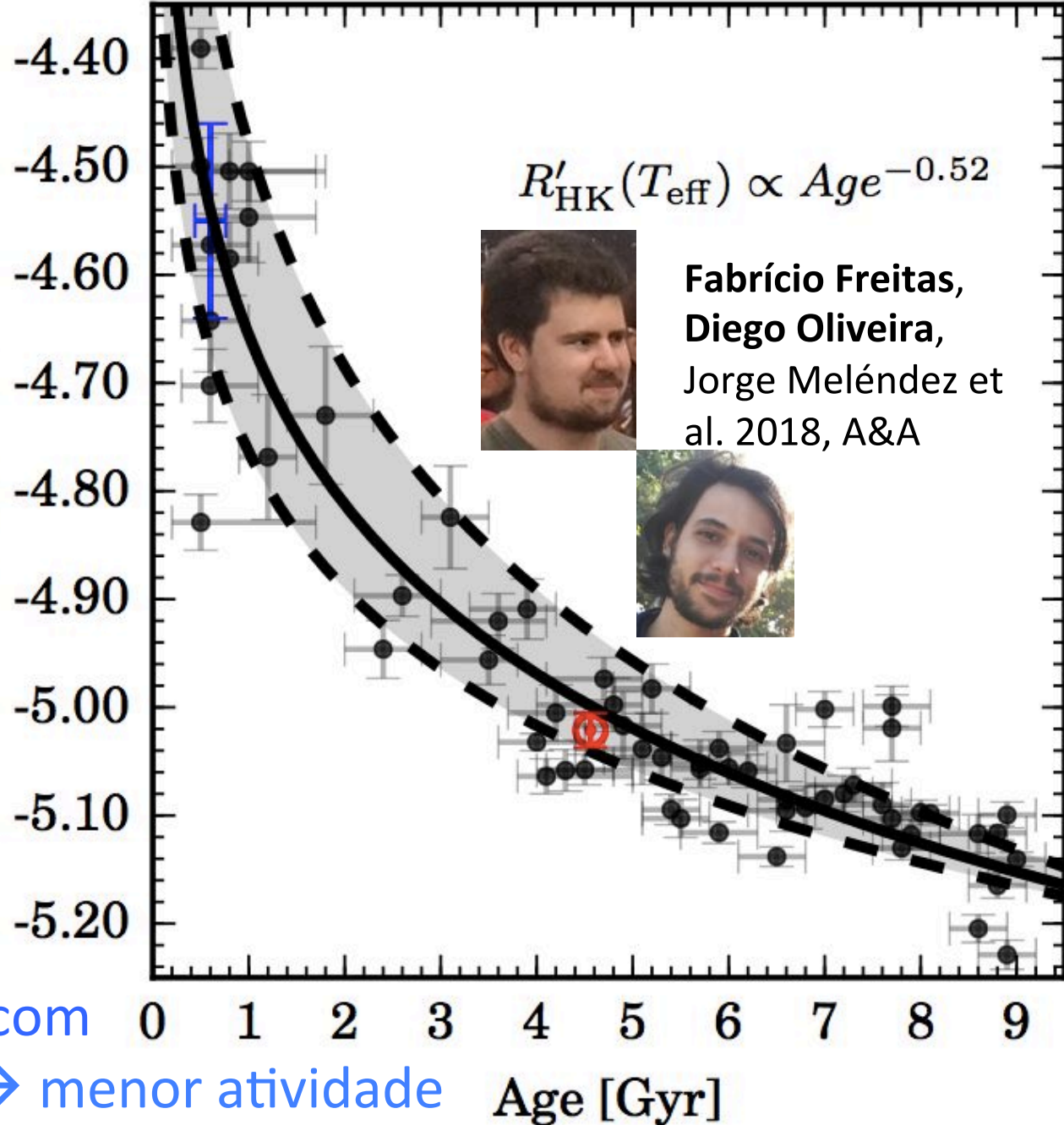


Ciclo de atividade usando o índice cromosférico S



Variações de atividade estelar em gêmeas solares na sequência principal (escala de bilhões de anos).

Índice de atividade R'_{HK} (depende do S)
 $\log R'_{\text{HK}}(T_{\text{eff}})$



Rotação mais lenta com aumento da idade → menor atividade

No índice R'_{HK} a contribuição fotosférica é subtraída → mais sensível à atividade cromosférica

Diferentes escalas de atividade estelar (dia – anos – bilhões de anos)

- Flutuações rápidas (< 1 dia), explosões (*flares*), proeminência solar eruptiva, ejeção de massa coronal (CME)
- Ciclo de atividade estelar (\sim anos), como o ciclo de 11 anos do Sol.
- Diminuição da atividade durante a sequência principal (escalas de milhões a bilhões de anos): estrelas jovens são muito ativas, estrelas velhas são mais calmas.

Provinha 10

- 1) Why the observed solar flux is higher at the maximum of the solar sunspot cycle
- 2) Explain briefly the 3 timescales of solar activity:
(A) days, (B) 11 years, (C) billions of years

Extra slides

- More detailed cartoons on the evolution of the magnetic field during the magnetic activity cycle, from the paper by Sanchez et al. 2014, An. Acad. Bras. Ciênc. vol.86 no.1:

A mean-field Babcock-Leighton solar dynamo model with long-term variability

http://www.scielo.br/scielo.php?script=sci_arttext&pid=S0001-37652014000100011

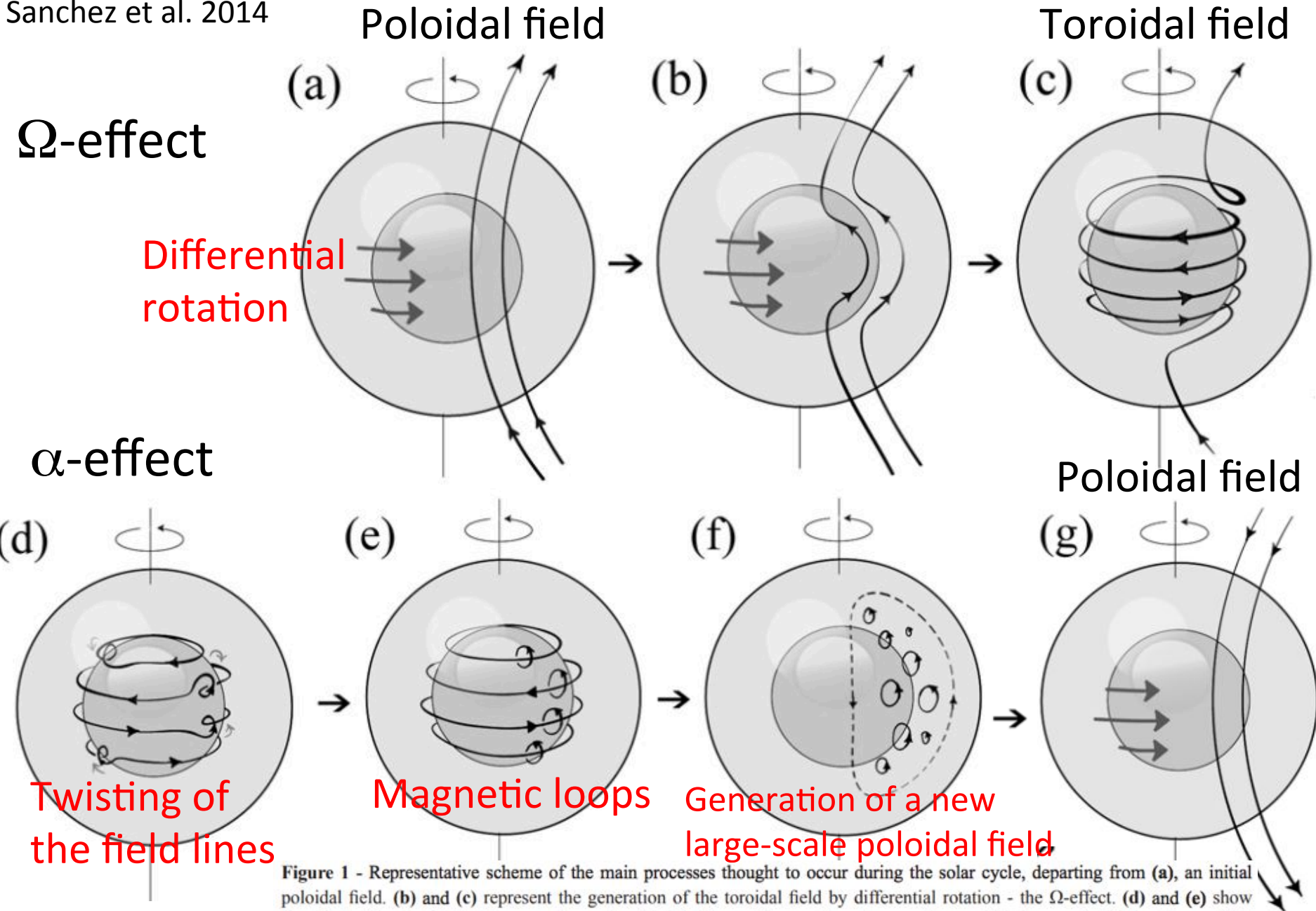


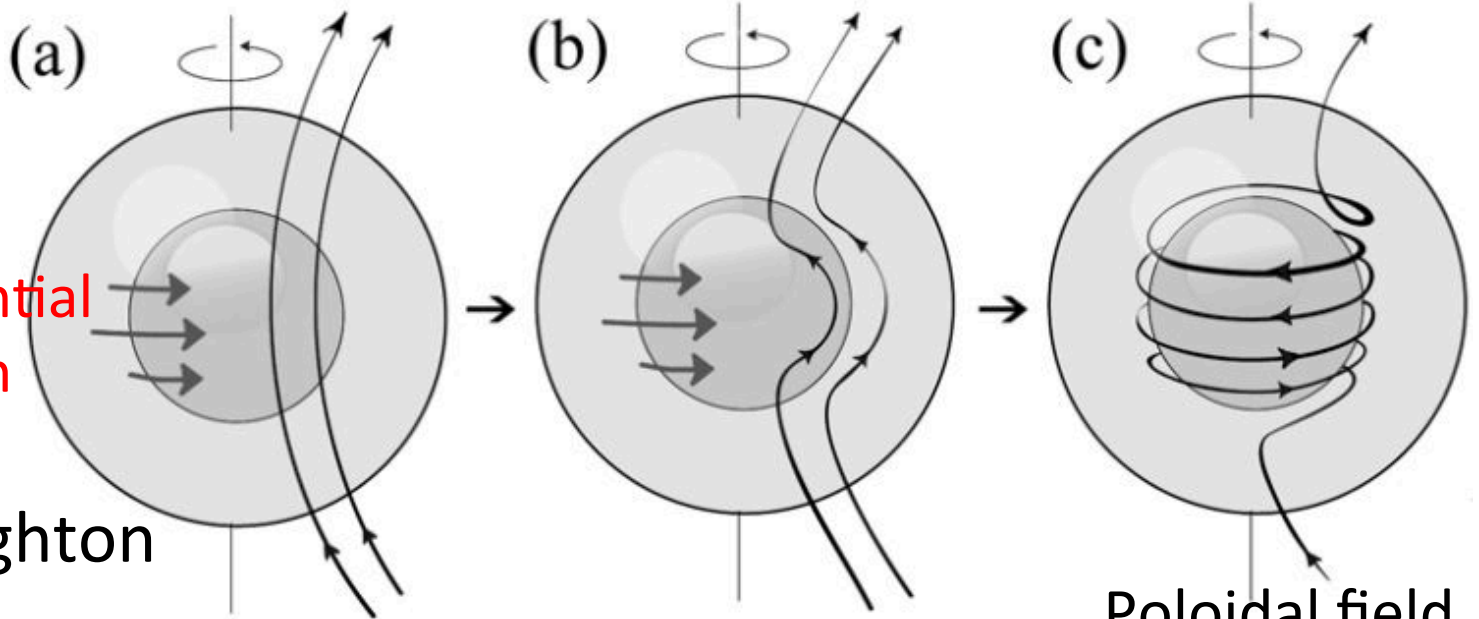
Figure 1 - Representative scheme of the main processes thought to occur during the solar cycle, departing from (a), an initial poloidal field. (b) and (c) represent the generation of the toroidal field by differential rotation - the Ω -effect. (d) and (e) show the effect of cyclonic turbulence on former toroidal fields, creating small-scale secondary poloidal magnetic fields - the α -effect. Averaged, they result in a net electromotive force generating a new large-scale poloidal field (f), closing the first half part of the magnetic cycle with a new poloidal field (g), with opposite polarity than the initial one. (h) represents the beginning of the Babcock-

Poloidal field

Toroidal field

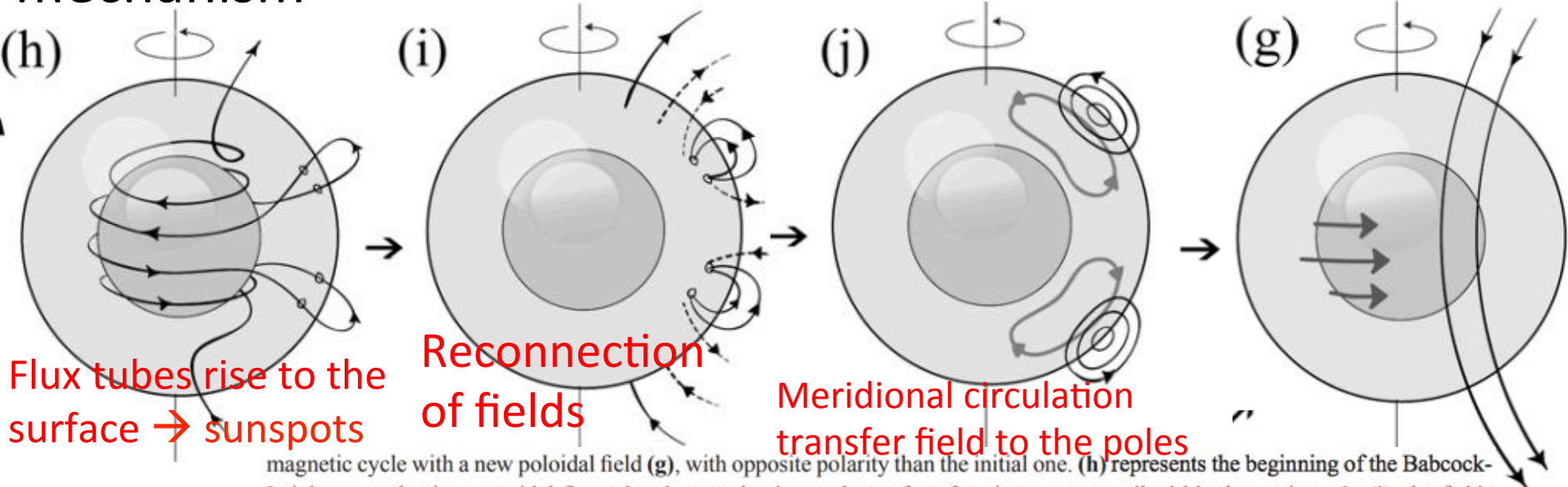
Ω -effect

Differential rotation



Babcock-Leighton mechanism

Poloidal field



Flux tubes rise to the surface \rightarrow sunspots

Reconnection of fields

Meridional circulation transfer field to the poles

magnetic cycle with a new poloidal field (g), with opposite polarity than the initial one. (h) represents the beginning of the Babcock-Leighton mechanism: toroidal flux tubes buoyantly rise to the surface forming sunspots, tilted bipolar regions. In (i), the fields from the bipolar regions diffuse and reconnect with each other and with the polar fields. The resulting poloidal flux is advected by meridional circulation to the poles (j), generating the final large-scale poloidal field in (g).